Subband Adaptive Filtering Using Approximately Alias-free Cosine Modulated Filterbanks

Student : Yin-Shao Chang Advisor : Yuan-Pei Lin

Department of Electrical and Control Engineering
National Chiao Tung University

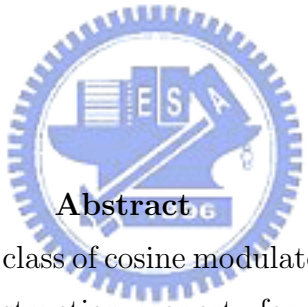

Abstract

In this paper, we use a class of cosine modulated filterbank (CMFB) with approximately reconstruction property for subband adaptive filtering. We show that even after the subband filters are included, the CMFB maintains the approximately alias-free property. In earlier designs, when the filterbank has real coefficients, the alias-free property is usually destroyed after subband filters are inserted. The CMFB has real coefficients and the computational complexity for filtering and subband adaptation is less than that of complex-valued filterbanks. Numerical simulations will be given to demonstrate its approximately alias-free property and fast convergence.

Contents

List of Figures

Chapter 1

Introduction

The subband adaptive filtering technique is very attractive for many applications, such as system identification, adaptive equalization, and acoustic echo cancelation, especially for systems with a long impulse response. We first describe acoustic echo cancelation by the teleconference system as follows. Teleconference system is shown in Fig. 1.1. The speech of the remote user is transmitted to the local user terminal, and vice versa. Both the microphone and the speaker are set in the room, so not only the speech of the local user but also that of the remote user, are transmitted to the remote terminal. Here we call the speech of the remote user which is transmitted back to the remote terminal, the acoustic echo. The echo can be generated by passing the speech of the remote user through the echo path. The estimated echo path is modeled as $h(n)$ in Fig. 1.1. As the echo path is estimated, then we can generate the echo $y(n)$ by passing the speech of the remote user through echo path. Subtracting the echo from the signal which is transmitted back to remote terminal, then the acoustic echo is canceled.

For example, in the application of acoustic echo cancelation, as referring to Fig, 1.2, we call the system impulse response $s(n)$ the echo path. The echo path usually has several thousands of taps. If we apply conventional fullband adaptive filtering [1], it is necessary to model the echo path by using a filter with several thousand taps. Computational burden is costly. Besides, the non-flatness of the input speech signal slows down the convergence speed [1].

Subband adaptive filtering is proposed in [2]. There are two advantages by

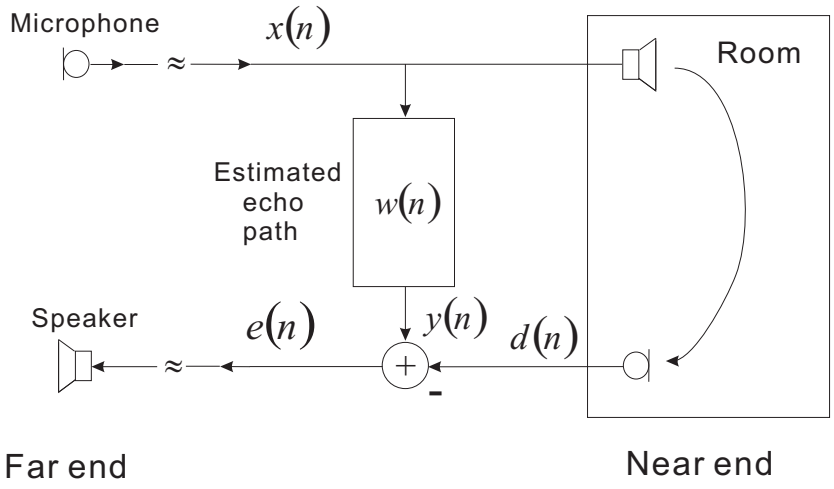

Figure 1.1: Teleconference system.

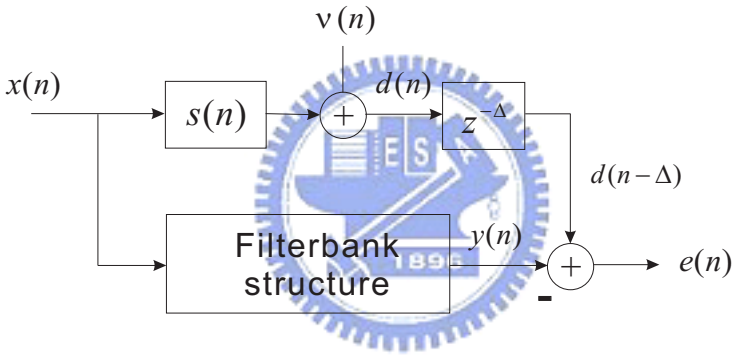

Figure 1.2: The general block diagram for echo cancelation by using multirate struture.

using subband adaptive structure. One is computation reduction, and the other is convergence speed improvement. Since the adaptation is processed after the downsampling M operation, the subband filters work at the reduced sampling rate, and then the computation of adaptation can be reduced by a factor of M. Furthermore, by using subband adaptation, we divide fullband signal process into several subband signals processing. Therefore, in each subband, the nonflatness of the input speech signal spectrum can be degraded. If M is large enough, then the spectrum for each subband is approximately flat.

The method which is not oversmapled but cross-filters needed is proposed in

[3] for modelization with small output errors. An optimal design of filterbank [4] is used to minimize mean-squared error (MSE) introduced by the aliasing components of the output signal, the error of distortion function from unity, and finite stopband attenuation of the analysis filterbank. After that, there are many prototype filter design methods based on the DFT or cosine modulated filterbank structure proposed. In [5], given the analysis and synthesis filters, an linear optimization method adjusts the prototype filter of the synthesis filterbank to minimize output error by LMS algorithm. An design [6] introduces the complex-valued and real-valued near perfect reconstruction NPR oversampled filterbank, designed by iteratively least-squares algorithm. A series of designs of oversampled uniform DFT filterbanks with different constraints, such as delay specification, inband aliasing reduction, and group delay specifications, are listed in [7] - [9]. The problem of aliasing effect and amplitude distortion are studied and prototype filters are sought by the nonliear programming technique [10].

In this paper, we apply the filterbank design method [11] and the prototype filter design method [12], constructing the cosine-modulated filterbank (CMFB), to achieve subband adaptive filtering . DFT filterbank structure are formed by the complex-valued analysis and synthesis filters, so the signal processing is performed with complex value. If we apply the subband filters following the expander and preceding the decimator, the filters are complex-valued. On the contrary, for CMFB, all analysis filters and synthesis filters are real-valued, so only real-valued computation is required. Therefore, all the signal processing is real-valued performed. The computational burden can be saved. Moreover, as shown later, the numerical simulation demonstrates the fast convergence speed.

1.1 Outline

- Chapter 2: The basic structure of subband adaptive structure, such as filterbank structure, the relationship between input, subband, and output signals, and adaptation algorithm is presented.

- Chapter 3: We survey two subband adaptive structures, such as Block DFT

and near perfect reconstruction filterbank (NPRFB). Block DFT has alias-free property property in Sec. 3.1. In Sec. 3.2, we introduce the NPRFB, as implied by the name, which has the property of near perfect reconstruction.

- Chapter 4: The proposed CMFB design method is described. In Sec. 4.1, given a prototype filter, we design CMFB, and observe its alias suppression. We review the Kaiser window approach for the design of prototype filter for CMFB in Sec. 4.2. In Sec. 4.3, we continue to examine the alias suppression when the subband adaptive filters are taken into consideration. With proper choice of subband filters, the proposed subband adaptive CMFB are approximately alias-free.

- Chapter 5: Performance measurements are presented, such as minimum mean-square error (MMSE), signal-to-alias ratio (SAR), modeling error (ME), and reconstruction error (RE). These measurements will be demonstrated in the next section.

- Chapter 6: In Sec. 6.1, we demonstrate the designed prototype filter and adjust the parameter of CMFB to observe the characteristics of the filterbank. Compare the experimental results of CMFB with those of the other investigated methods for the environment with different SNR levels in Sec. 6.2.

- Chapter 7: Conclusion.

1.2 Notations

1. The lower-case letters represent scalar values.

2. The lower-case and upper-case letters with bold face represent vector and matrix quantities.

3. W_M is defined as $e^{-j2\pi/M}$.

4. $\mathbf{A}^\dagger$ denotes transpose-conjugate of $\mathbf{A}$.

5. The notation $\mathbf{I}_M$ is used to represent the $M \times M$ identity Matrix.

6. The notation $diag(\lambda_1, \lambda_2, \cdots, \lambda_L)$denotes an $M \times M$ diagonal matrix with the diagonal element equal to λ_k.

7. The notation $\mathbf{W}_M$ is used to represent the normalized $M \times M$ DFT matrix given be

$$[\mathbf{W}_M]_{kn} = \frac{1}{\sqrt{M}} e^{-j\frac{2\pi}{M}kn}$$

where $0 \leq k, n \leq M-1$.

Chapter 2

Subband Adaptive Structure

There are two advantages by using subband adaptive structure. One is computation reduction, and the other is convergence speed improvement. Since the adaptation is processed after the downsampling M operation, the subband filters work at the reduced sampling rate, and then the computation of adaptation can be reduced by a factor of M. Furthermore, by using subband adaptation, we divide fullband signal process into several subband signals processing. Therefore, in each subband, the nonflatness of the input speech signal spectrum can be degraded. If M is large enough, then the spectrum for each subband is approximately flat.

2.1 The expression of input, subband, and output signals

As shown in Fig. 2.1, $H_k(z)$ and $F_k(z)$, are the analysis filters and synthesis filters, for $0 \leq k \leq K-1$. We derive an input-output expression for the multirate structure. In this structure, the input signal $x(n)$ is filtered by the analysis filters $H_k(z)$ in the kth subband, decimated by a factor M, and resulting in the subband signals $x_k(n)$. The subband signals can be expressed as

$$X_k(z) = \frac{1}{M} \sum_{\ell=0}^{M-1} H_k(z^{1/M} W_M^{\ell}) X(z^{1/M} W_M^{\ell}),\ 0 \leq k \leq K-1 \qquad (2.1)$$

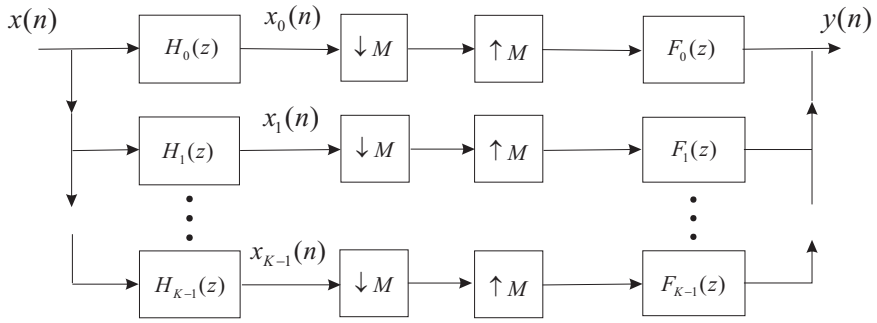

Figure 2.1: Filterbank structure with K subbands and downsampling factor M.

Then the subband signals are interpolated by the factor M, filtered by the synthesis filters $F_k(z)$, and added together to form the output signal $y(n)$.

$$Y(z) = \frac{1}{M} \sum_{\ell=0}^{M-1} \sum_{k=0}^{K-1} H_k(zW_M^{\ell}) F_k(z) X(zW_M^{\ell}) \tag{2.2}$$

We define the transfer function $T_\ell(z)$ as

$$T_\ell(z) = \frac{1}{M} \sum_{k=0}^{K-1} H_k(zW_M^{\ell}) F_k(z) \tag{2.3}$$

where $T_0(z)$ is the distortion transfer function, and $T_\ell(z), 1 \leq \ell \leq M-1$ is the aliasing transfer function.With the definition above, the output signal is then expressed as

$$Y(z) = \sum_{\ell=0}^{M-1} T_\ell(z) X(zW_M^{\ell}) \tag{2.4}$$

If the aliasing terms are approximately zero or approximately alias-free, i.e.,

$$T_\ell(z) \approx 0, \ \forall \ 1 \leq \ell \leq M-1 \tag{2.5}$$

Then simplify (2.4) to

$$Y(z) \approx T_0(z) X(z) \tag{2.6}$$

Furthermore, if the output signal is essentially a copy of the input signal with some delay Δ, i.e., $y(n) \approx cx(n-\Delta)$, where c is a constant, then we say that such a filterbank possesses perfect reconstruction (PR) or near perfect reconstruction (NPR) property.

Both the transfer function and the alias function depend on the analysis filters $H_k(z)$ and synthesis filters $F_k(z)$. The analysis filters and synthesis filters are generated by one or two prototype filters. Under this structure, the design of the prototype filter properly is of importance to achieve the PR or NPR property.

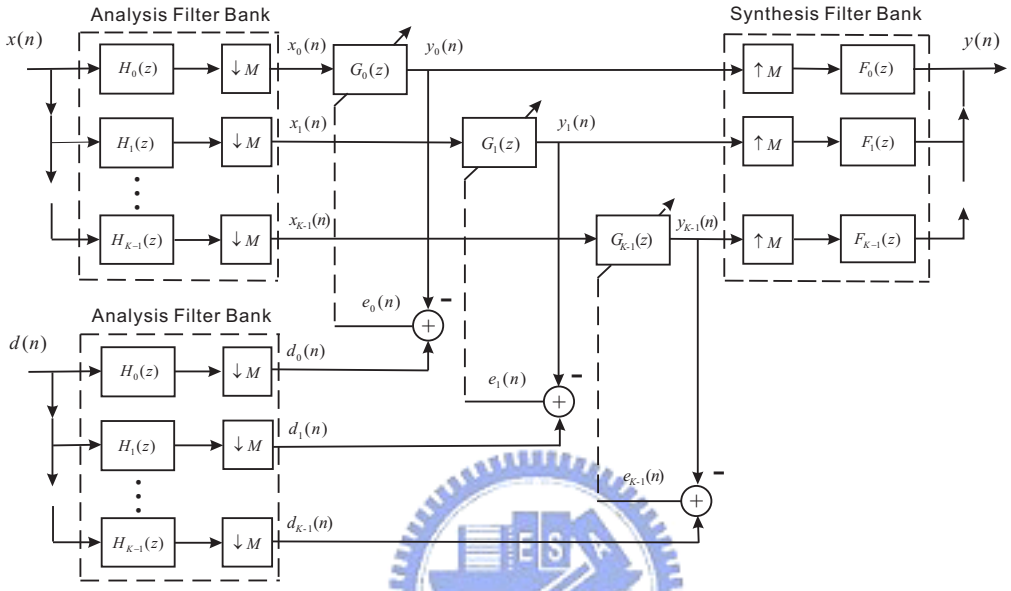

Figure 2.2: Subband adaptive filtering structure.

Consider the filterbank structure with subband adaptive filters $G_k(z)$, as shown in Fig. 2.2. $d(n)$ is the fullband desired signal. We apply an analysis filterbank with the input $d(n)$ to generate the desired signal for the training of the subband filters. The transfer function from $x(n)$ to $y(n)$, defined in (2.3) now becomes

$$T_\ell(z) = \frac{1}{M}\sum_{k=0}^{K-1} H_k(zW_M^\ell)F_k(z)G_k(z^M) \tag{2.7}$$

Given analysis filterbank and synthesis filterbank, we adapt $G_k(z)$ by using LMS algorithm to make the overall transfer function from $x(n)$ to $y(n)$ similar to the echo path.

2.2 Adaptation algorithm

The adaptive filter coefficients are derived using normalized LMS algorithm. The LMS algorithm is known for its simplicity of implementation, that is, the update equation depends on the input signal and the error signal between the reference signal and the output signal. Even through it is shown that the asymptotic convergence rate is generally slow, being at best of order one over sample time for bandlimited white noise [13].

Suppose the kth subband filter $g_k(n)$ has L_k coefficients, written in the vector form as

$$\mathbf{g}_k(n) = [g_{k,0}(n) \quad g_{k,1}(n) \quad \cdots \quad g_{k,L_k-1}(n)]^T. \tag{2.8}$$

The input vector, or regressor, is of the form

$$\mathbf{x}_k(n) = [x_k(n) \quad x_k(n-1) \quad \cdots \quad x_k(n-L_k+1)]^T. \tag{2.9}$$

The update equation of the coefficient of the subband filter based on the normalized LMS algorithm is

$$\mathbf{g}_k(n+1) = \mathbf{g}_k(n) + \frac{\mu}{p_k(n)}\mathbf{x}_k(n)e_k^{\dagger}(n) \tag{2.10}$$

where the error signal $e_k(n)$

$$\begin{aligned} e_k(n) &= d_k(n) - y_k(n) \\ y_k(n) &= \mathbf{g}_k^{\dagger}(n)\mathbf{x}_k(n) \end{aligned} \tag{2.11}$$

where $y_k(n)$ is the output signal of the kth subband filter $g_k(n)$. $p_k(n)$ is the normalization factor which depends on the regressor. Hence, $\mu/p_k(n)$ becomes a time-varying stepsize. When the regressor has large power, the time-varying stepsize will become smaller to prevent divergence; when the regressor has smaller power, the time-varying stepsize will be larger to accelerate the convergence speed. Furthermore, for each subband, the stepsize will be adjusted automatically according to the regressor. We can use $p_k(n)$ with the expression

$$p_k(n) = \epsilon + \|\mathbf{x}_k(n)\|^2 \tag{2.12}$$

with a positive constant ϵ to avoid division by zero or by a small number when the regressor is zero or close to zero. Another choice for the normalization factor is

$$p_k(n) = \beta p_k(n-1) + (1-\beta)\|\mathbf{x}_k(n)\|^2 \quad , 0 \leq \beta \leq 1. \tag{2.13}$$

Taking the expected value on the both sides of the above equation, we get

$$E\{p_k(n)\} = \beta E\{p_k(n-1)\} + (1-\beta)E\{\|\mathbf{x}_k(n)\|^2\}. \tag{2.14}$$

As the time index n approaches infinity, $E\{p_k(n)\} \rightarrow E\{p_k(n-1)\}$, therefore

$$E\{p_k(n)\} \rightarrow E\{\|\mathbf{x}_k(n)\|^2\} \tag{2.15}$$

We call $p_k(n)$ the power estimation of the regressor $x_k(n)$ [14]. These two normalization factors will be used later in the numerical simulation to ensure the convergence of the adaptation.

Chapter 3

A survey of subband adaptive filtering using DFT FB

In this section, we focus on the uniform DFT filterbank, whose analysis filters and synthesis filters are shifted versions of the lowpass prototype filter, i.e.,

$$H_k(z) = H_0(zW_K^k),\ F_k(z) = F_0(zW_K^k) \tag{3.1}$$

with $0 \leq k \leq K-1$, where $H_0(z)$ and $F_0(z)$ are analysis and synthesis prototype filters.

Next, we will introduce two oversampled filterbank structures. One is the Block DFT [15]. We derive an equivalent system of an LTI system $S(z)$ by the filterbank structure with subband filters. The other is the near perfect reconstruction (NPR) oversampled filterbank [6]. The design criterion is based on the minimization of the reconstruction error of the filterbank and the stopband attenuation of the prototype filter. Using this designed prototype filter, we can construct a filterbank with the near perfect reconstruction property.

3.1 Block DFT [15]

Fullband signal processing us that signals are processed on a sample-by-sample basis. See Fig. 3.1, the output sequence $y(i)$ is the convolution of the input sequence $u(n)$ and system impulse response $s(n)$, that is, expressed in z-domain

$$Y(z) = S(z)U(z) \tag{3.2}$$

where $Y(z) = \sum_{n=0}^{\infty} y(n)z^{-n}$, $S(z) = \sum_{n=0}^{L-1} s(n)z^{-n}$, and $U(z) = \sum_{n=0}^{\infty} u(n)z^{-n}$. Block signal processing is that signals are processed on block-by-block basis. We divide the input sequence into several blocks. Each block contains M samples. So do the output sequence. The block diagram is shown in Fig. 3.2.

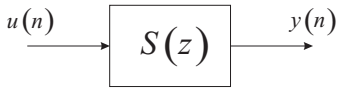

Figure 3.1: Full-band signal processing.

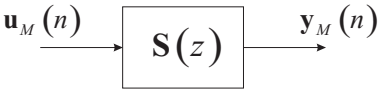

Figure 3.2: Block signal processing.

The equivalent transfer function $\mathbf{S}(z)$ between the blocked version of input signal $\mathbf{u}_M(n)$ and the blocked version of output signal $\mathbf{y}_M(n)$ is of the form of a pseudo-circulant matrix

$$\mathbf{S}(z) = \begin{pmatrix} P_0(z) & P_1(z) & \cdots & P_{M-1}(z) \\ z^{-1}P_{M-1}(z) & P_0(z) & \ddots & P_{M-2}(z) \\ \vdots & \ddots & \ddots & \vdots \\ z^{-1}P_1(z) & z^{-1}P_2(z) & \cdots & P_0(z) \end{pmatrix}_{M\times M} \tag{3.3}$$

where $P_k(z)$, for $0 \le k \le M-1$, are M polyphase components of $S(z)$.

The following derives the result that the equivalent transfer function $\mathbf{S}(z)$ can be decomposed as the product of two matrices, $\widetilde{\mathbf{P}}(z)$ and $\widetilde{\mathbf{Q}}(z)$. Define $\mathbf{P}(z)$ and $\mathbf{Q}(z)$ as

$$\mathbf{P}(z) = \begin{pmatrix} P_0(z) & P_1(z) & \cdots & P_{M-1}(z) & 0 & \cdots & 0 \\ 0 & \ddots & \ddots & \ddots & \ddots & \ddots & \vdots \\ \vdots & \ddots & \ddots & \ddots & \ddots & \ddots & 0 \\ 0 & \cdots & 0 & P_0(z) & P_1(z) & \cdots & P_{M-1}(z) \end{pmatrix}_{M\times(2M-1)} \tag{3.4}$$

$$\mathbf{Q}(z) = \begin{pmatrix} \mathbf{I_M} \\ z^{-1}\mathbf{I_{M-1}} \quad \mathbf{0} \end{pmatrix}_{(2M-1)\times M} \tag{3.5}$$

Moreover, define $\widetilde{\mathbf{P}}(z)$ and $\widetilde{\mathbf{Q}}(z)$ which are modified from $\mathbf{P}(z)$ and $\mathbf{Q}(z)$

$$\widetilde{\mathbf{P}}(z) = \begin{pmatrix} P_0(z) & P_1(z) & \cdots & P_{M-1}(z) & 0 & \cdots & \cdots & 0 \\ 0 & \ddots & \ddots & \ddots & \ddots & \ddots & \ddots & \vdots \\ \vdots & \ddots & \ddots & \ddots & \ddots & \ddots & \ddots & \vdots \\ 0 & \cdots & 0 & P_0(z) & P_1(z) & \cdots & P_{M-1}(z) & 0 \end{pmatrix}_{M\times 2M} \tag{3.6}$$

$$\widetilde{\mathbf{Q}}(z) = \begin{pmatrix} \mathbf{I_M} \\ z^{-1}\mathbf{I_M} \end{pmatrix}_{2M\times M} \tag{3.7}$$

such that

$$\mathbf{S}(z) = \widetilde{\mathbf{P}}(z)\widetilde{\mathbf{Q}}(z) \tag{3.8}$$

Furthermore, decompose $\widetilde{\mathbf{P}}(z)$ as a constant matrix and a circulant matrix $\mathbf{C}(z)$

$$\widetilde{\mathbf{P}}(z) = \begin{pmatrix} \mathbf{I}_M & \mathbf{0}_{M\times M} \end{pmatrix} \mathbf{C}(z) \tag{3.9}$$

where

$$\mathbf{C}(z) = \begin{pmatrix} P_0(z) & P_1(z) & \cdots & P_{M-1}(z) & 0 & \cdots & \cdots & 0 \\ 0 & \ddots & \ddots & \ddots & \ddots & \ddots & & \vdots \\ \vdots & & & & \ddots & & & \vdots \\ & & & P_0(z) & P_1(z) & \cdots & P_{M-1}(z) & \\ 0 & & & & & & & P_{M-1}(z) \\ P_{M-1}(z) & & & & & & & \vdots \\ \vdots & \ddots & & & & & & \vdots \\ P_1(z) & \cdots & P_{M-1}(z) & 0 & \cdots & \cdots & 0 & P_0(z) \end{pmatrix}_{2M\times 2M} \tag{3.10}$$

By using the fact that the circulant matrix can be diagonalized by the normalized DFT matrix $\mathbf{W}$

$$\mathbf{C}(z) = \mathbf{W}^{\dagger}\mathbf{\Lambda}(z)\mathbf{W} \tag{3.11}$$

for some diagonal matrix $\mathbf{\Lambda}(z)$ with elements $G_k(z)$, for $0 \le k \le 2M-1$. It can be shown that

(a) Assume the length of system impulse response L can be divided by M. Each subfilter $G_k(z)$ is an FIR transfer function with L/M coefficients and

(b) The polyphase components $P_k(z)$, for $0 \le k \le M-1$, can be obtained by the linear combination of the subfilters $G_k(z)$, for $0 \le k \le 2M-1$. That is,

$$\begin{pmatrix} P_0(z) & \cdots & P_{M-1}(z) & \mathbf{0}_{1\times M} \end{pmatrix}^T = \mathbf{W} \begin{pmatrix} G_0(z) & G_1(z) & \cdots & G_{2M-1}(z) \end{pmatrix}^T \tag{3.12}$$

Substitute (3.8) with (3.9) and (3.11)

$$\mathbf{S}(z) = \begin{pmatrix} \mathbf{I}_M & \mathbf{0}_{M\times M} \end{pmatrix} \mathbf{W}^\dagger \mathbf{\Lambda}(z) \mathbf{W} \widetilde{\mathbf{Q}}(z) \tag{3.13}$$

Proof:

(a) From $\mathbf{C}(z) = \mathbf{W}^\dagger \mathbf{\Lambda}(z) \mathbf{W}$, by multiplying $\mathbf{W}$ and $\mathbf{W}^\dagger$, we can get

$$\mathbf{\Lambda}(z) = \mathbf{W}\mathbf{C}(z)\mathbf{W}^\dagger \tag{3.14}$$

That is, $G_k(z)$ is the linear combination of $\{P_k(z)\}_{k=0}^{M-1}$. In addition, each polyphase components of $G(z)$, $\{P_k(z)\}_{k=0}^{M-1}$, has L/M coefficients, so does $G_k(z)$.

(b) By taking transpose on $\mathbf{C}(z) = \mathbf{W}^\dagger \mathbf{\Lambda}(z) \mathbf{W}$, we can get

$$\mathbf{C}(z)^T = \mathbf{W}^T \mathbf{\Lambda}(z) \mathbf{W}^* \tag{3.15}$$

Multiplying a column vector $\begin{pmatrix} 1 & 0 & \cdots & 0 \end{pmatrix}^T$ on both sides, then

$$\begin{aligned}
\text{LHS} &= \mathbf{C}(z)^T \begin{pmatrix} 1 \\ 0 \\ \vdots \\ 0 \end{pmatrix} \\
&= \begin{pmatrix} P_0(z) \\ \vdots \\ P_{M-1}(z) \\ \mathbf{0}_{1\times B} \end{pmatrix} \\
\text{RHS} &= \mathbf{W}^T \mathbf{\Lambda}(z) \mathbf{W}^* \begin{pmatrix} 1 \\ 0 \\ \vdots \\ 0 \end{pmatrix} \\
&= \mathbf{W}^T \mathbf{\Lambda}(z) \begin{pmatrix} 1 \\ 1 \\ \vdots \\ 1 \end{pmatrix} \\
&= \mathbf{W} \begin{pmatrix} G_0(z) \\ G_1(z) \\ \vdots \\ G_{2M-1}(z) \end{pmatrix}
\end{aligned} \tag{3.16}$$

Therefore

$$\begin{pmatrix} P_0(z) \\ \vdots \\ P_{M-1}(z) \\ \mathbf{0}_{B\times 1} \end{pmatrix} = \mathbf{W} \begin{pmatrix} G_0(z) \\ G_1(z) \\ \vdots \\ G_{2M-1}(z) \end{pmatrix} \tag{3.17}$$

It should be pointed out that although any diagonal matrix $\mathbf{\Lambda}(z)$ will always result in a circulant matrix $\mathbf{C}(z)$, it does not guarantee that any such $\mathbf{\Lambda}(z)$ will result in a circulant matrix that has the special form of (3.12). Therefore, we can modify the subband filters by the following rule for each iteration and get the subband filters which satisfy the constraint defined in (3.12).

$$\begin{pmatrix} G_0^c(z) \\ G_1^c(z) \\ \vdots \\ G_{2M-1}^c(z) \end{pmatrix} = \mathbf{W}^\dagger \begin{pmatrix} \mathbf{I_M} & \\ & \mathbf{0_{M\times M}} \end{pmatrix} \mathbf{W} \begin{pmatrix} G_0(z) \\ G_1(z) \\ \vdots \\ G_{2M-1}(z) \end{pmatrix} \tag{3.18}$$

where the superscript c means the constraint. By using (3.13), we can construct the equivalent system on the block-by-block basis in Fig. 3.3. The time domain equivalent system with the oversampled filterbank structure is shown in Fig. 3.4.

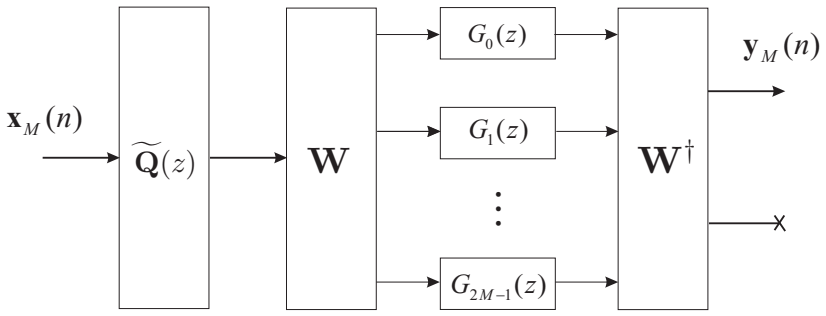

Figure 3.3: An equivalent system structure on the block-by-block.

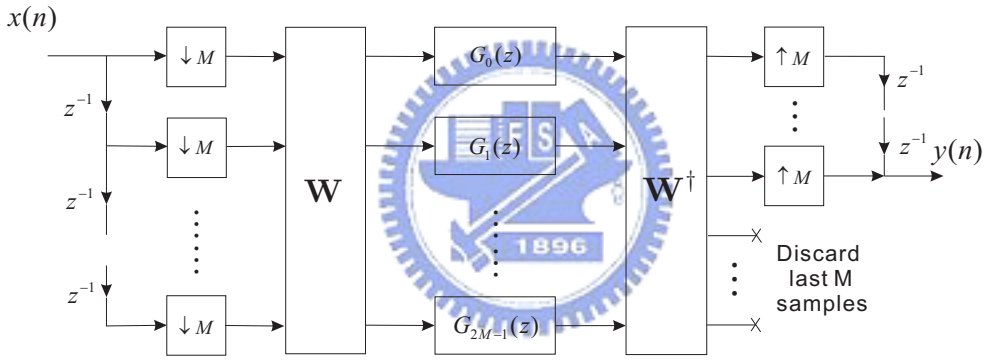

Figure 3.4: The time domain equivalent system with the oversampled filterbank structure.

3.2 NPR Oversampled filterbank [6]

The following is the description of the design of the complex-valued oversampled filterbank. We divide this section into two paragraphs, derivation of filterbank and design of prototype filter.

Given a real-valued linear phase prototype filter $p(n)$, the analysis filters are derived from $p(n)$ by a generalized discrete Fourier transform (GDFT)

$$h_k(n) = p(n)\exp\{j\tfrac{2\pi}{K}(k+0.5)(n+n_0)\} \quad , 0 \le k \le K-1 \tag{3.19}$$

A time offset $n_0 = -(\ell_p - 1)/2$ ensures linear phase analysis filters provided that the prototype filter $p(n)$ is linear phase. The length of the prototype filter ℓ_p is assumed to be even. With the selection as the time reversal of the analysis filters, the synthesis filters are of the form

$$f_k(n) = \widetilde{h}_k(n) = h_k(n) \tag{3.20}$$

The frequency offset 0.5 affects the position of the passband of $H_k(z)$.

To design the oversampled filterbank, the performance criterion ξ to be minimized is the combination of the filterbank reconstruction error and the stopband energy of the prototype filter.

$$\xi = \xi_1 + \gamma^2 \xi_2 \tag{3.21}$$

where γ^2 is the positive weighting factor. We describe ξ_1 and ξ_2 as follows.

A. Reconstruction Error

If the aliasing is small enough to be neglected, the impulse response of the filterbank $t_0(n)$, as defined in (2.3), can be written as a convolution of the analysis filters and synthesis filters

$$\begin{aligned} t_0(n) &= \tfrac{1}{M} \sum_{k=0}^{K-1} h_k(n) * h_k(n) \\ &= \tfrac{1}{M} \sum_{k=0}^{K-1} t_{0,k}(n) \end{aligned} \tag{3.22}$$

The $t_{0,k}(n)$ can be formulated as a vector $\mathbf{t}_{0,k}$ which contain $2\ell_p - 1$ samples of $t_{0,k}(n)$

$$\begin{aligned} \mathbf{t}_{0,k} &= \begin{pmatrix} t_{0,k}(0) \\ t_{0,k}(1) \\ \vdots \\ t_{0,k}(2\ell_p - 2) \end{pmatrix} \\ &= \begin{pmatrix} h_k(0) & 0 & \cdots & 0 \\ h_k(1) & h_k(0) & \cdots & 0 \\ \vdots & \ddots & & \vdots \\ 0 & 0 & \cdots & h_k(\ell_p - 1) \end{pmatrix} \begin{pmatrix} f_k(0) \\ f_k(1) \\ \vdots \\ f_k(\ell_p - 1) \end{pmatrix} \\ &= \mathbf{H}_k \mathbf{f}_k \end{aligned} \tag{3.23}$$

The synthesis filters $f_k(n)$ are derived from the prototype filter $p(n)$, so the vector $\mathbf{f}_k$ can be written as

$$\mathbf{f}_k = \mathbf{M_k p} \tag{3.24}$$

where $\mathbf{p}$ contains all coefficients of the prototype filter $p(n)$ and $\mathbf{M_k}$ is a diagonal matrix with elements

$$[\mathbf{M_k}]_{nn} = \exp\{j\frac{2\pi}{K}(k+0.5)(n+n_0)\} \tag{3.25}$$

The vector form $\mathbf{t}_0$ of impulse response $t_0(n)$ of the filterbank can be expressed as

$$\mathbf{t}_0 = \frac{1}{M}\sum_{k=0}^{K-1}\mathbf{H}_k\mathbf{M_k p} \tag{3.26}$$

The measurement for reconstruction error ξ_1 is then expressed as the square of the norm of the difference between the vector $\mathbf{t}_0$ and a vector $\mathbf{v}$ which represents a delay

$$\xi_1 = \|\mathbf{t}_0 - \mathbf{v}\|^2 = \left\|\frac{1}{M}\sum_{k=0}^{K-1}\mathbf{H}_k\mathbf{M_k p} - \mathbf{v}\right\|^2 \tag{3.27}$$

Here, the meaning of the reconstruction error is to make the distortion function approach to a pure delay by design of the prototype filter.

B. Stopband energy of the prototype filter

The stopband energy of the prototype filter can be evaluated by the frequency response of the prototype filter at the frequency points $\{\omega_0, \omega_1, \cdots, \omega_N\}$ covering the whole stopband.

$$\begin{aligned}\xi_2 &= \left\| \begin{pmatrix} 1 & \cos(\omega_0\cdot 1) & \cdots & \cos(\omega_0\cdot \ell_p - 1) \\ 1 & \cos(\omega_1\cdot 1) & \cdots & \cos(\omega_1\cdot \ell_p - 1) \\ \vdots & \ddots & & \vdots \\ 1 & \cos(\omega_N\cdot 1) & \cdots & \cos(\omega_N\cdot \ell_p - 1) \end{pmatrix} \begin{pmatrix} p(0) \\ p(1) \\ \vdots \\ p(\ell_p - 1) \end{pmatrix} \right\|^2 \\ &= \|\mathbf{\Omega p}\|^2 \end{aligned} \tag{3.28}$$

Therefore, the performance criterion ξ now becomes

$$\xi = \left\| \begin{pmatrix} \frac{1}{M}\sum_{k=0}^{K-1}\mathbf{H}_k\mathbf{M_k} \\ \gamma\mathbf{\Omega} \end{pmatrix}\mathbf{p} - \begin{pmatrix} \mathbf{v} \\ \mathbf{0} \end{pmatrix} \right\|^2 \tag{3.29}$$

In addition, the prototype filter has linear phase property, so we only need to design half of coefficients of the prototype filter. The vector $\mathbf{p}$ is then of the form

$$\mathbf{p} = \begin{pmatrix} \mathbf{I}_{\ell/2} \\ \mathbf{J}_{\ell/2} \end{pmatrix} \mathbf{p}_{0.5} = \mathbf{L}\mathbf{p}_{0.5} \tag{3.30}$$

where $\mathbf{J}$ represents the inverse identity matrix and $\mathbf{p_{0.5}}$ is the vector form of half coefficients of $p(n)$. The criterion becomes

$$\xi = \left\| \mathbf{A}\mathbf{p}_{0.5} - \begin{pmatrix} \mathbf{v} \\ \mathbf{0} \end{pmatrix} \right\|^2 \tag{3.31}$$

where

$$\mathbf{A} = \begin{pmatrix} \frac{1}{M} \sum_{k=0}^{K-1} \mathbf{H}_k \mathbf{M_k} \mathbf{L} \\ \gamma \mathbf{\Omega} \mathbf{L} \end{pmatrix} \tag{3.32}$$

The criterion to be minimized becomes a least-squares problem. We can apply the iterative least-squares algorithm. The minimization algorithm is listed in the following table. Step 3 can be achieved by the QR decomposition for $\mathbf{A}$.

Iterative Least-Squares Design Algorithm

Step	Command
1	initial $p(0)$, set $i = 1$
2	construct $\mathbf{A}(i)$ from $p(i-1)$
3	minimize the criterion with respect to $p(i)$
4	apply relaxation $p(i) = \tau p(i) + (1-\tau)p(i-1)$
5	if $\|p(i) - p(i-1)\| < \epsilon$ then stop else $i = i+1$, goto 2

Chapter 4

Proposed Method-CMFB

In this section, we review the design of the approximately alias-free CMFB. Given the prototype filter design, we can construct an oversampled filterbank. When the subband filters are taken into consideration, the CMFB has approximately alias-free property as long as we choose the subband filter with the symmetric rule, which will be mentioned in a later section. Then we design the prototype filter by the Kaiser window approach. With property design criterion, the subband adaptive CMFB is approximately alias-free.

4.1 CMFB with approximate reconstruction [11]

In the DFT filterbank, the analysis and synthesis filters have complex coefficients. The CMFB comes into play if real coefficients are desired. In this section, we review the oversampled cosine modulated filterbank. Consider an oversampled CMFB with $2M$ subbands and decimation ratio M.

Let $P(z)$ be the prototype filter of the analysis filterbank, and we take $\widetilde{P}(z)$ as that of the synthesis filterbank, where $\widetilde{P}(z)$ is the time-reversal version. Let $P_k(z) = P(zW_{2M}^{k+0.5})$, $0 \leq k \leq 2M-1$. The analysis filters $H_k(z)$ and the synthesis filters $F_k(z)$ are given by

$$\begin{aligned} H_k(z) &= \begin{cases} P_k(z) + P_{2M-1-k}(z) & ,0 \leq k \leq M-1 \\ -jP_k(z) + jP_{2M-1-k}(z) & ,M \leq k \leq 2M-1 \end{cases} \\ F_k(z) &= \widetilde{H}_k(z) \qquad\qquad ,0 \leq k \leq 2M-1 \end{aligned} \tag{4.1}$$

when all $H_k(z)$ and $F_k(z)$ have real coefficients. As the CMFB is real-valued, the signal processing is implemented by the real-valued addition and multiplication. It is shown in [11] that if $|P(e^{j\omega})|^2$ is a Nyquist (2M) filter satisfying $P(e^{j\omega}W_{2M}^{2\ell})\widetilde{P}(e^{j\omega}) \approx 0$, for $1 \leq \ell \leq M-1$, then the CMFB has the approximate reconstruction property.

4.2 Proposed subband adaptive CMFB

In the following, we calculate the aliasing transfer function (2.3) to investigate the approximately alias-free property with subband filters for CMFB. For convenience, we move the subband filters to the synthesis filterbank. Now we focus on the kth subband to observe how the alias is generated.

As the input signal passing through the analysis filter $H_k(z)$, the filtered signal has the frequency component in the spectral support of $H_k(z)$, as shown in Fig. 4.1(a). Due to decimation following the expansion, both $P_k(z)$ and $P_{2M-1-k}(z)$ have $M-1$ image copies. Referring to Fig. 4.1(b), $M-3$ image copies of $P_k(z)$ fall into the stopband of $P_{2M-1-k}(z)$, provided that $P(z)$ has stopband edge less than π/M. However, two image copies of $P_k(z)$ overlap with the spectral support of $\widetilde{P}_{2M-1-k}(z)$. As these two signal components pass through synthesis filters, alias comes out.

The solution to this problem without subband filters is proposed in [11]. Here we want to find the proper choice of the subband filters so that aliasing error will be canceled after the subband filters are included. The derivation is shown as follows. Substitute the designed CMFB in (4.1) to (2.7)

$$\begin{aligned} T_\ell(z) &= \tfrac{1}{M}\sum_{k=0}^{2M-1} H_k(zW_M^\ell)F_k(z)G_k(z^M) \\ &= \tfrac{1}{M}\sum_{k=0}^{M-1}(P_k(zW_{2M}^{2\ell}) + P_{2M-1-k}(zW_{2M}^{2\ell}))(\widetilde{P}_k(z) + \widetilde{P}_{2M-1-k}(z))G_k(z^M) \\ &\quad + \tfrac{1}{M}\sum_{k=M}^{2M-1}(-jP_k(zW_{2M}^{2\ell}) + jP_{2M-1-k}(zW_{2M}^{2\ell}))(j\widetilde{P}_k(z) - j\widetilde{P}_{2M-1-k}(z))G_k(z^M) \end{aligned} \tag{4.2}$$

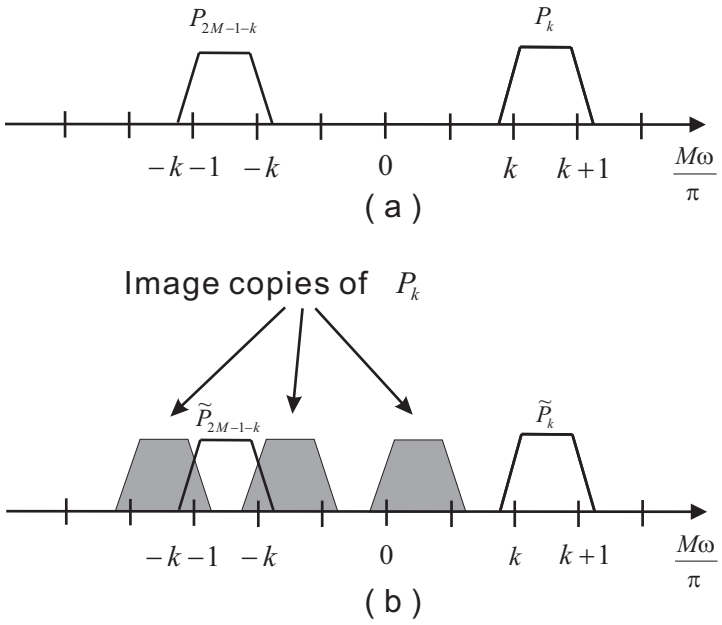

Figure 4.1: The diagram of the aliasing generation for cosine modulated fiterbank.

For simplicity, we have used P_k as a shorthand for $P_k(z)$. Then

$$\begin{aligned}
T_\ell(z) &= \tfrac{1}{M}\sum_{k=0}^{M-1}(P_{k+2\ell}\widetilde{P}_k + P_{k+2\ell}\widetilde{P}_{2M-1-k} + P_{2M-1-k+2\ell}\widetilde{P}_k + P_{2M-1-k+2\ell}\widetilde{P}_{2M-1-k})G_k(z^M) \\
&\quad + \tfrac{1}{M}\sum_{k=M}^{2M-1}(P_{k+2\ell}\widetilde{P}_k - P_{k+2\ell}\widetilde{P}_{2M-1-k} - P_{2M-1-k+2\ell}\widetilde{P}_k + P_{2M-1-k+2\ell}\widetilde{P}_{2M-1-k})G_k(z^M) \\
&= \tfrac{1}{M}\sum_{k=0}^{M-1}(P_{k+2\ell}\widetilde{P}_k + P_{k+2\ell}\widetilde{P}_{2M-1-k} + P_{2M-1-k+2\ell}\widetilde{P}_k + P_{2M-1-k+2\ell}\widetilde{P}_{2M-1-k})G_k(z^M) \\
&\quad + \tfrac{1}{M}\sum_{k'=0}^{M-1}(P_{2M-1-k'+2\ell}\widetilde{P}_{2M-1-k'} - P_{2M-1-k'+2\ell}\widetilde{P}_{k'} - P_{k'+2\ell}\widetilde{P}_{2M-1-k'} + P_{k'+2\ell}\widetilde{P}_{k'}) \\
&\quad \cdot G_{2M-1-k'}(z^M)
\end{aligned} \tag{4.3}$$

If we choose the subband filters by the rule

$$G_k(z) = G_{2M-1-k}(z),\ 0 \le k \le M-1 \tag{4.4}$$

Then the aliasing transfer function becomes

$$\begin{aligned} T_\ell(z) &= \tfrac{1}{M}\sum_{k=0}^{M-1}(P_{k+2\ell}\widetilde{P}_k + P_{2M-1-k+2\ell}\widetilde{P}_{2M-1-k})G_k(z^M) \\ &\quad + \tfrac{1}{M}\sum_{k=0}^{M-1}(P_{k+2\ell}\widetilde{P}_k + P_{2M-1-k+2\ell}\widetilde{P}_{2M-1-k})G_{2M-1-k}(z^M) \\ &= \tfrac{2}{M}\sum_{k=0}^{M-1}(P_{k+2\ell}\widetilde{P}_k + P_{2M-1-k+2\ell}\widetilde{P}_{2M-1-k})G_k(z^M) \end{aligned} \tag{4.5}$$

If $P(e^{j\omega})$ satisfies

$$P(e^{j\omega}W_{2M}^{2\ell})\widetilde{P}(e^{j\omega}) \approx 0, \text{ for } 1 \le \ell \le M-1 \tag{4.6}$$

as shown in Fig. 4.2, then total aliasing error is approximately zero. Furthermore,

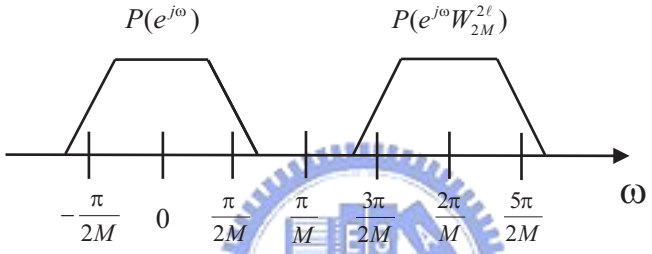

Figure 4.2: The condition of approximately alias-free property.

setting $\ell = 0$, we can get the overall distortion transfer function $T(e^{j\omega})$ as

$$T(e^{j\omega}) = \frac{2}{M}\sum_{k=0}^{2M-1}\left|P_k(e^{j\omega})\right|^2 G_k(e^{jM\omega}). \tag{4.7}$$

From the derivation above, if the condition stated in (4.6) holds, the appearance of the subband filters do not destroy the approximately alias-free property for CMFB. The choice of the subband filters in (4.4) means that only half the subband filters need to be adapted.

Block DFT and NPRFB are formed by complex-valued analysis and synthesis filters, so complex-valued computation is required. On the contrary, since CMFB has real-valued analysis, the subband signals are real, so are the coefficients of the subband adaptive filter. The signal processing is implemented by the real-valued addition and multiplication. The computation complexity is saved for filtering and subband adaptation.

4.3 Prototype filter design

From the discussion in the previous section, we can know that the condition for approximate reconstruction can be stated in terms of $P(e^{j\omega})$ as follows

$$P(e^{j\omega}) \approx 0 \ \ , \ \text{for} \, |\omega| > \pi/M \tag{4.8}$$

which is equivalent to (4.6) and

$$|T(e^{j\omega})| \approx 1 \tag{4.9}$$

where

$$T(e^{j\omega}) = \sum_{k=0}^{2M-1} \left|P(e^{j(\omega - k\pi/M)})\right|^2 \tag{4.10}$$

Fig. 4.3 illustrates the magnitude response of the prototype filter.

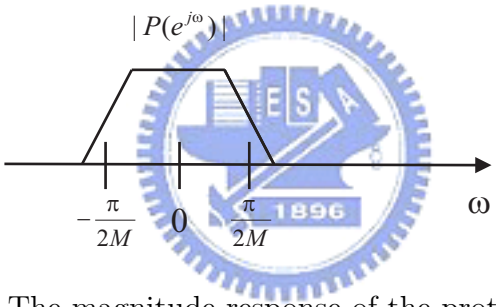

Figure 4.3: The magnitude response of the prototype filter.

Here we apply Kaiser window design method to design the prototype filter [16]. The filter $p(n)$ of length $N+1$ is of the form

$$p(n) = h(n)v(n) \tag{4.11}$$

where

$$h(n) = \frac{sin(\omega_c(n - 0.5N))}{\pi(n - 0.5N)} \tag{4.12}$$

is the impulse response of the ideal filter with cutoff frequency ω_c and $v(n)$ is the Kaiser window, given by

$$v(n) = \begin{cases} I_0[\beta\sqrt{1-(n/0.5N)^2}]/I_0(\beta), & -N/2 \le n \le N/2 \\ 0, & \text{otherwise.} \end{cases} \tag{4.13}$$

where $I_0(x)$ is the modified zero-order Bessel function. which can be computed from

$$I_0(x) = 1 + \sum_{k=1}^{\infty} \left[\frac{(0.5x)^k}{k!} \right]^2 \tag{4.14}$$

The parameter β depends on the attenuation specification A_s of the low pass filter. The quantity β is found from

$$\beta = \begin{cases} 0.1102(A_s - 8.7), & \text{if } A_s > 50 \\ 0.5842(A_s - 21)^{0.4} + 0.07886(A_s - 21), & \text{if } 21 \leq A_s \leq 50 \\ 0, & \text{if } A_s < 21 \end{cases} \tag{4.15}$$

Given the stop attenuation A_s and transition bandwidth $\Delta\omega$, the filter order N is estimated by

$$N \approx \frac{A_s - 7.95}{14.36\Delta\omega/2\pi} \tag{4.16}$$

With A_s and $\Delta\omega$, the only free parameter for design of the prototype filter is the cutoff frequency ω_c. Given the performance criterion ϕ,we can design the prototype filter to find the extreme value of ϕ by adjusting ω_c. The following description reviews the prototype filter design method proposed in [12].

Define a filter $G(e^{j\omega}) = |P(e^{j\omega})|^2$. Observe that the condition in (4.8) and (4.9) means that $G(e^{j\omega})$ is approximately a Nyquist (2M) filter. In other words, $g(2Mn)$ is approximately $1/2M\delta(n)$, where $\delta(n)$ is given by

$$\delta(n) = \begin{cases} 1 & n = 0 \\ 0 & \text{otherwise.} \end{cases} \tag{4.17}$$

Using this, we can choose a simpler objective function $\phi_{new} = \max_{n,n\neq 0} |g(2Mn)|$. We can adjust the parameter ω_c to find the prototype filter $p(n)$ that yields the smallest ϕ_{new}.

Chapter 5

Performance measurements

In this section, we will discuss four major measurements used in the following simulations. That is, MMSE (Minimum Mean-Squared Error), SAR (Signal-to-Alias Ratio), ME (Modeling Error), and RE (Reconstruction Error) [18].

A. MSE

In Fig. 1.2, we use the filterbank structure to estimate the echo path for the application of acoustic echo cancelation. One objective for subband adaptive filters is to minimize the error between the fullband signal reconstructed by the synthesis filterbank and the desired echo signal with a specific delay. That is,

$$\text{MSE} = E\{|d(n-\Delta) - y(n)|^2\}. \tag{5.1}$$

The mean-squared error is an important metric. We will show learning curve of MSE in the section of numerical simulation.

B. SAR

Given the prototype filter, SAR is defined as

$$\text{SAR} = \frac{\int_0^{\pi} \left|P(e^{j\omega})\right|^2 d\omega}{\int_{\pi/M}^{\pi} \left|P(e^{j\omega})\right|^2 d\omega} \tag{5.2}$$

which is a measure of the stopband energy of the prototype filter, which also determines the amount of aliasing.

C. ME

Referring to Fig. 5.1, if the impulse response of the echo path is $s(n)$, the echo path estimated by subband adaptive filtering is $w(n)$, then the modeling error is

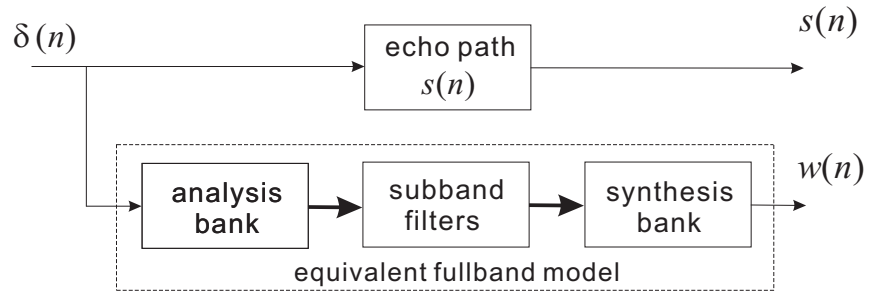

Figure 5.1: The block diagram of the system identification by using multirate struture.

defined as

$$\mathrm{ME} = \|w(n) - s(n)\|^2 \,/\, \|(s(n))\|^2 \tag{5.3}$$

If we focus on the system identification, The modeling error is an important metric for system identification application.

D. RE

Suppose the condition for approximately alias-free property holds, and the distortion function of the filterbank is expressed as $t_0(n)$. Then the reconstruction error is defined as

$$\mathrm{RE} = \|t_0(n) - \delta(n - \Delta)\|^2 \tag{5.4}$$

where Δ is a delay introduced by the filterbank. The purpose of design of the prototype filter is to make the distortion function approximately a delay. Therefore, RE is a measure of the degree how the distortion function approximates a delay.

Chapter 6

Numerical Simulations

Here we will apply the proposed subband adaptive CMFB to acoustic echo cancelation. The prototype has stopband attenuation 100dB and length 28. The echo path models we use are an impulse and an echo path adopted from ITU-T Recommendation G.168. These two echo path models will be used in the following simulation examples. The echo paths has 1024 taps. For the echo path G.168, its impulse response has two taps with significant value, as shown in Fig. . Its magnitude response and phase response are shown in Fig. 6.2. In this section, the oversampled filterbank has 4 subbands, that is, $M = 2$. Subband adaptive filters are of length 512. The input signal $x(n)$ is a first-order auto-regressive (AR) signal. The signal-to-noise ratio is 20dB, 30dB, 40dB and infinity (noise absent).

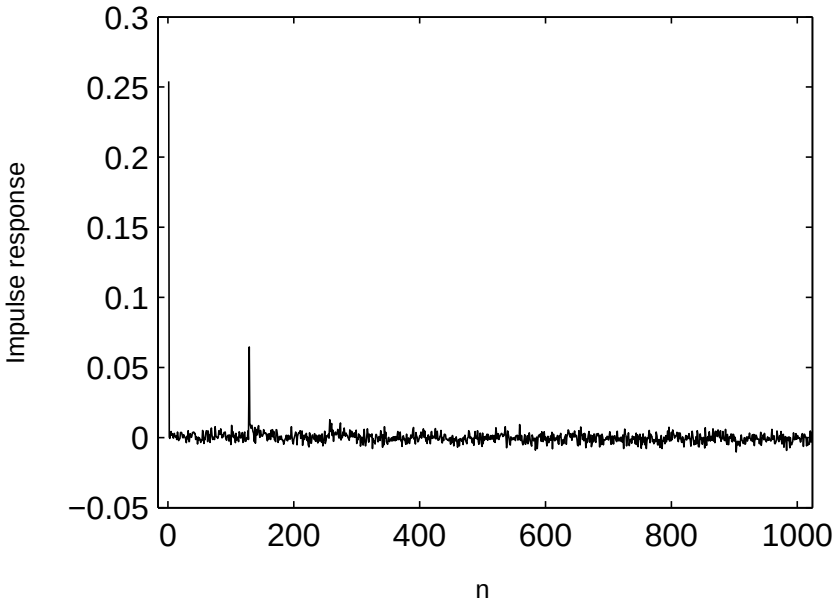

Figure 6.1: Impulse response of the echo path adopted from G.168.

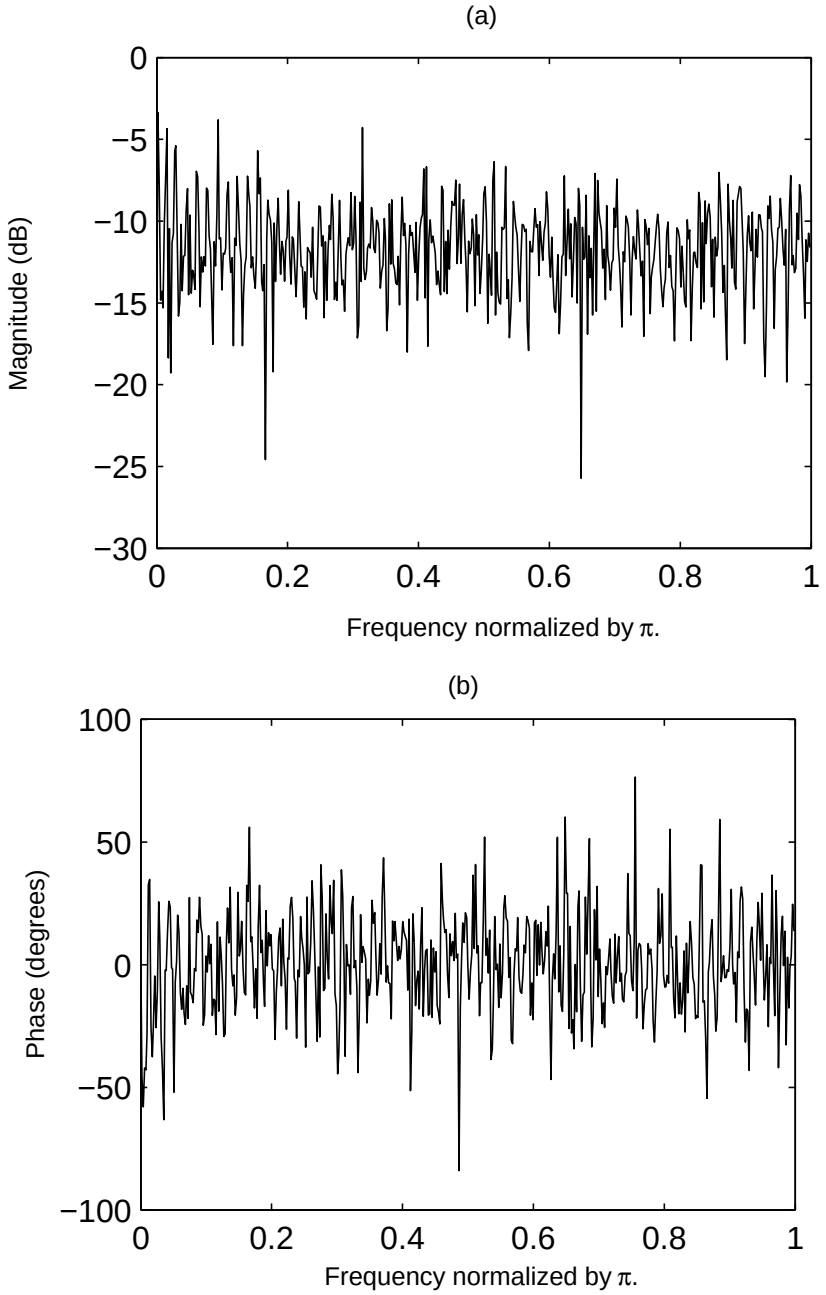

Figure 6.2: (a) Magnitude response and (b) phase response of the echo path adopted from G.168.

6.1 Prototype filter design and the characteristics of the proposed filterbank

Since the design strategy of the filterbank comes from the one or two prototype filters, the prototype filter design has vital effect on the performance of the subband adaptive filterbank. According to the design algorithm as mentioned before, we plot the magnitude response of the prototype filter for NPRFB and CMFB, as shown in Fig. 6.3 and 6.4, respectively. All of them have linear phase property, so we only plot the magnitude response. For CMFB, the stopband attenuation is 100dB. The prototype filter is of length 28. Its SAR is 79.9628dB. For the NPRFB design method, we get the prototype filter with length 30. Its SAR is 107.8561dB. The cutoff frequency are both around $\omega = 0.5\pi$. Observing these two prototype filters, the stopband attenuation of CMFB is 100dB and that of NPRFB is about 100dB. Both of them satisfy the condition in (4.8) for their large stopband attenuation.

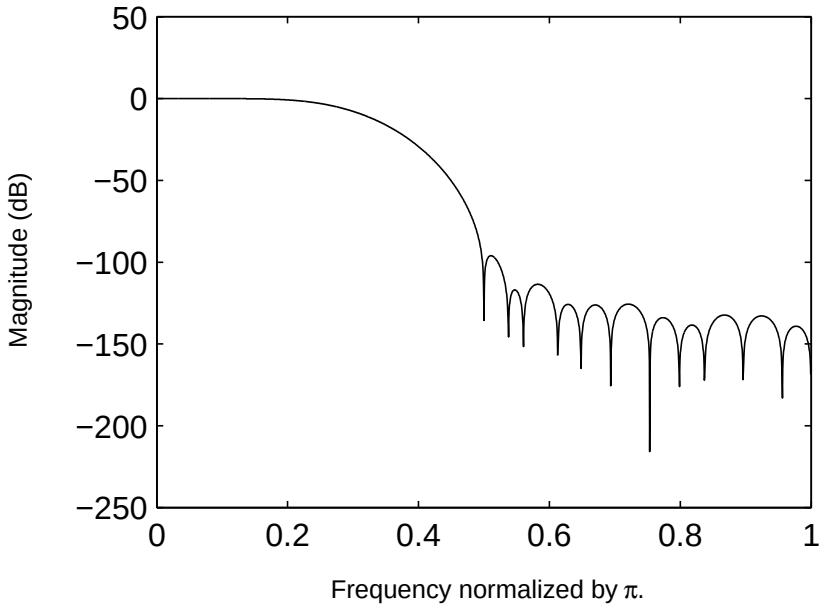

Figure 6.3: Magnitude response of prototype filter for NPRFB.

Next, we examine the characteristics of the filterbank, i.e, the distortion and

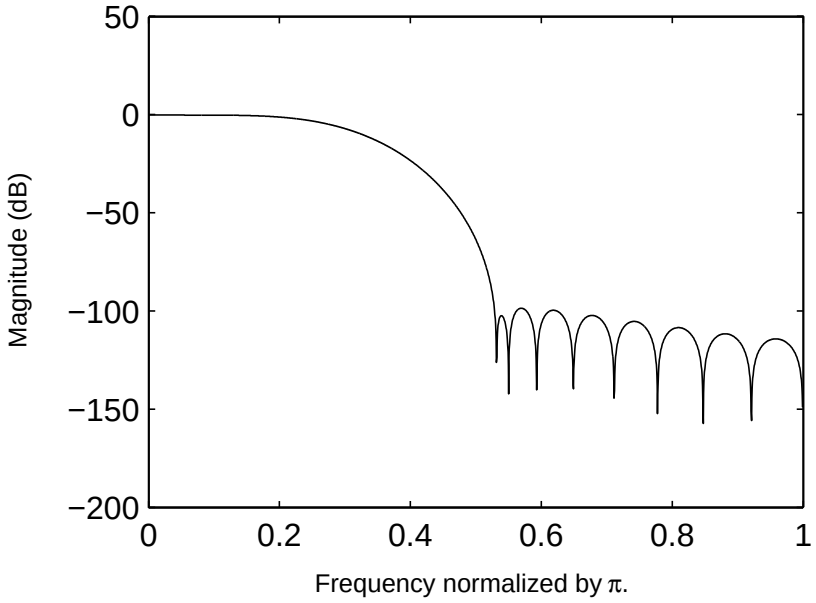

Figure 6.4: Magnitude response of prototype filter for CMFB.

alias suppression for the designed filterbank. As described in (4.9), we design the prototype filter $p(n)$ so that the distortion function $T_0(e^{j\omega})$ is as close to a unity delay as possible. Under the condition that aliasing is small enough to be neglected, this measurement $(1 - |T_0(e^{j\omega})|)^2$ can be viewed as a measure of reconstruction error. Here we call $(1 - |T_0(e^{j\omega})|)^2$ the distortion error. Since the distortion function defined in (4.10) has period π/M, we plot the distortion error $(1 - |T_0(e^{j\omega})|)^2$ for one period in Fig. 6.5 (a) for NPRFB and Fig. 6.6 (a) for CMFB, to observe the difference between the magnitude response of $T_0(e^{j\omega})$ and unity. The order of $(1 - |T_0(e^{j\omega})|)^2$ of NPRFB and CMFB are around 10^{-8} and 10^{-5}, respectively. All of them satisfies the condition in (4.9). Moreover, we compute RE by the impulse response $t_0(n)$. The RE of CMFB is -53.2829dB and that of NPRFB is -76.7095dB, respectively.

A measurement of aliasing error is [17]

$$\sqrt{\sum_{\ell=1}^{M-1} |T_\ell(e^{j\omega})|^2} \tag{6.1}$$

where $T_\ell(z)$ is the aliasing transfer function as defined in (2.3). The aliasing error

are shown in Fig. 6.5 (b) for NPRFB and Fig. 6.6 (b) for CMFB. The aliasing levels of the NPRFB and CMFB, are about -290dB to -300dB. Both of them are approximately alias-free.

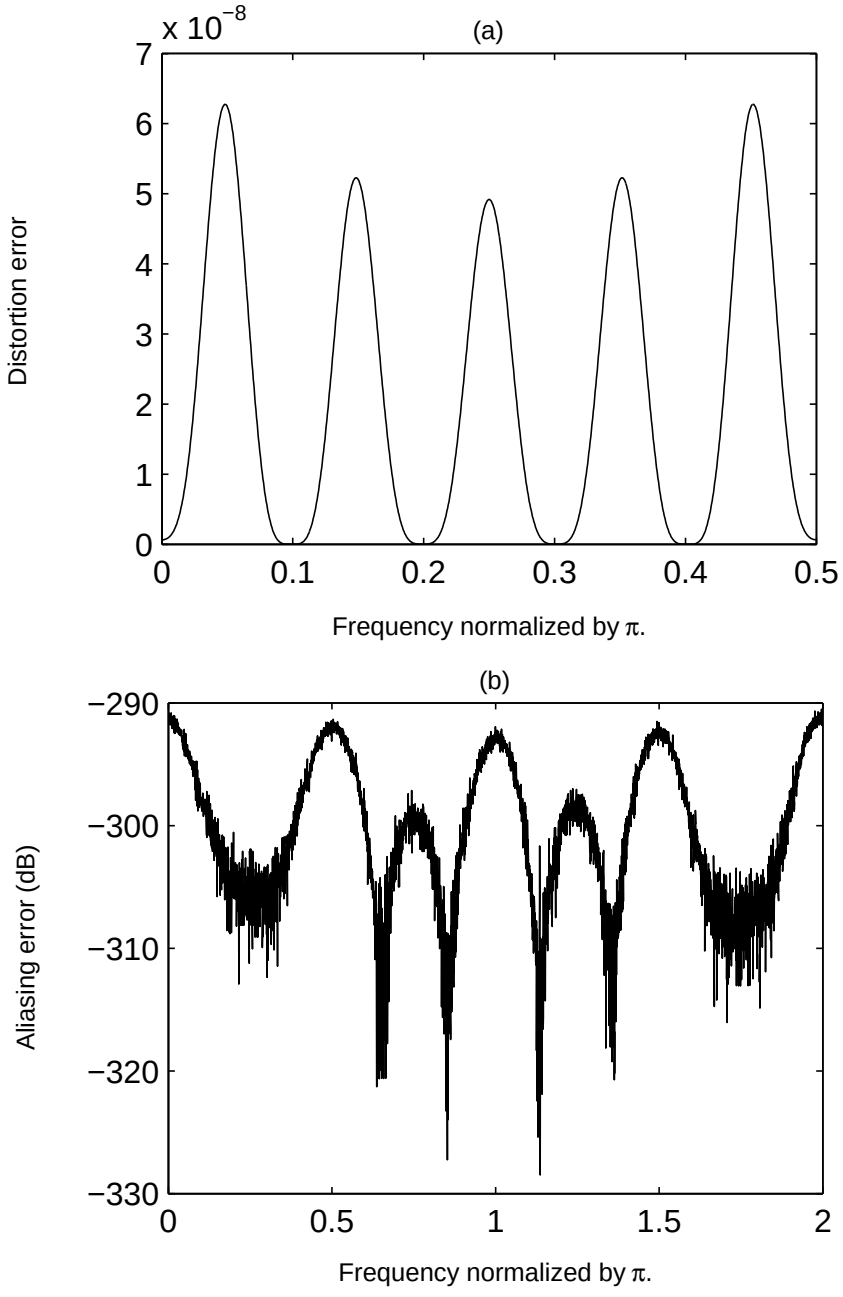

Figure 6.5: (a) Distortion error and (b) aliasing error of NPRFB.

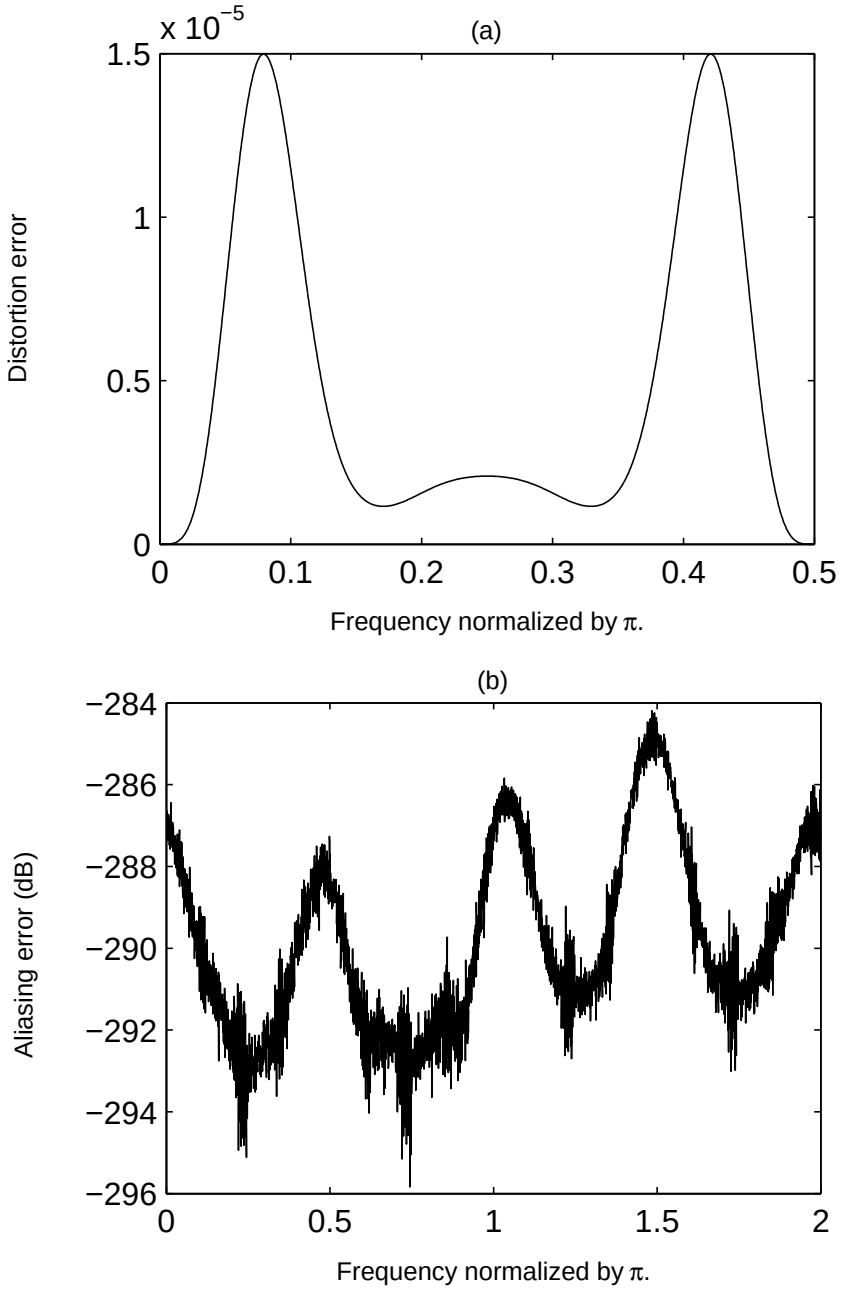

Figure 6.6: (a) Distortion error and (b) aliasing error of CMFB.

6.2 Parameter adjustments for CMFB

In the following, we adjust the parameter of CMFB to observe the characteristics of CMFB. In the design of prototypes, one parameter is the transition bandwidth $\Delta\omega$. Then we choose different initial value for the subband adaptive filter. Finally, we investigate the ability of the echo path estimation and the approximately alias-free property for CMFB.

We use different transition bandwidth to investigate the distortion function and aliasing transfer functions. Fig. 6.7 (a) shows the distortion of CMFB. For different transition bandwidth $\Delta\omega$, the distortion curves are similar. However, the aliasing measurements are quite different. All the aliasing measurements are all small enough to be neglected.

The initial condition of the subband adaptive filter can affect the convergence behavior. Here we change the initial condition of the subband adaptive filter to observe the MSE learning curve. The initial condition is that we take the multiple of the vector $\mathbf{q}$ with all elements equal to one as the subband adaptive filter. What we change is a constant which multiply with the vector $\mathbf{q}$. As shown in Fig. 6.8, if we choose the zero vector as the initial value of the subband adaptive filter, we can get the best learning curve. Therefore, we use the all zeros vector as the initial of the subband adaptive filter for the CMFB in the following example.

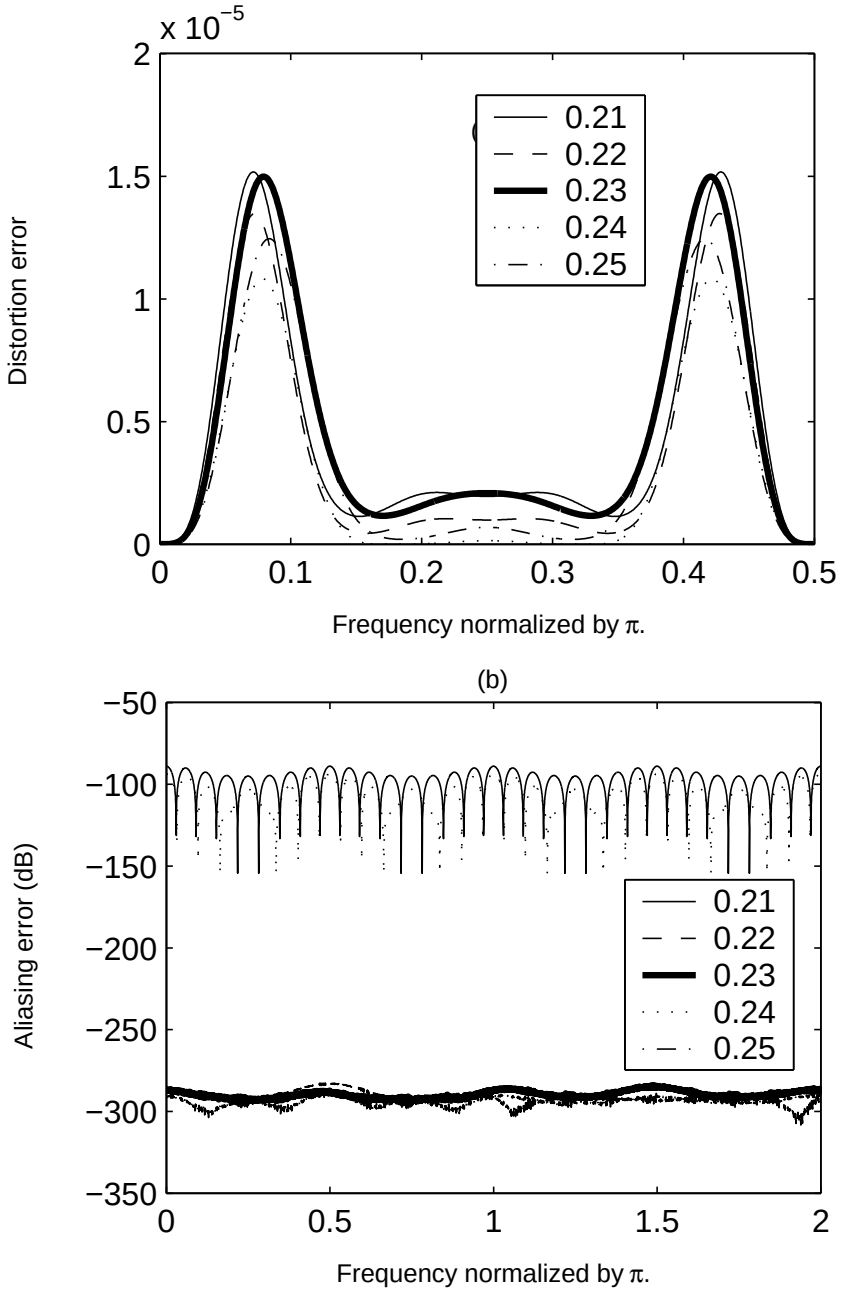

Figure 6.7: (a) The distortion and (b) the aliasing measurement with different transition bandwidth for CMFB.

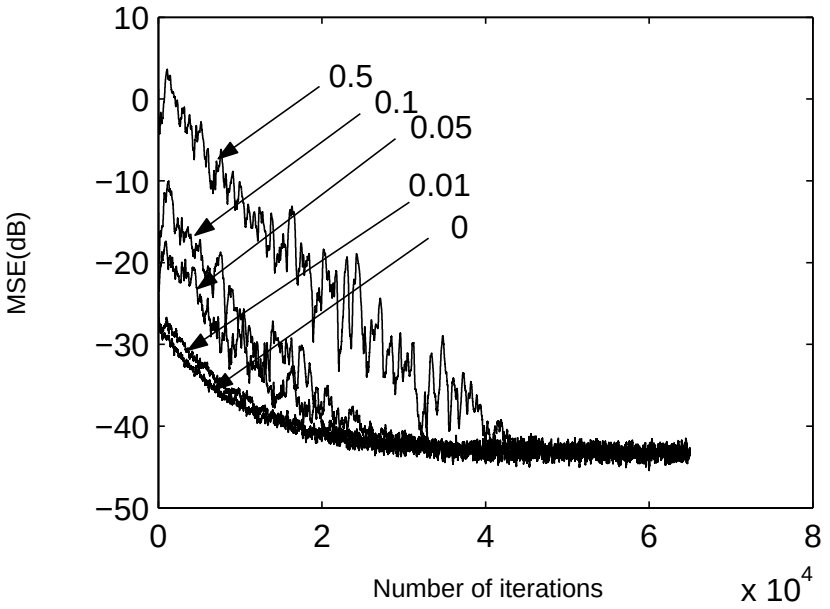

Figure 6.8: The learning curve for different choices of initial subband adaptive filters when the echo path is adopted from G.168.

6.3 Echo path modeling

We plot the original echo path model and the echo path model estimated for the impulse and G.168 by CMFB in Fig. 6.9 and Fig. 6.10. The estimated echo path is approximately a delay of the original one. Here the designed prototype filter is of order $N = 27$. If we zoom in the figure, the delay is indeed 27. The delay is introduced by the analysis and synthesis filters of CMFB. The delay can be estimated by the group delay introduced by the analysis filter and the synthesis filter, where N is the order of the prototype filter. The modeling errors are -48.494 dB and -18.753 dB for impulse echo path and G.168. Furthermore, we examine the alias measurement of CMFB with the inclusion of the subband adaptive filters in Fig. 6.11 and Fig. 6.12. We can see that aliasing error is approximately zero. The proposed subband adaptive CMFB is approximately alias-free.

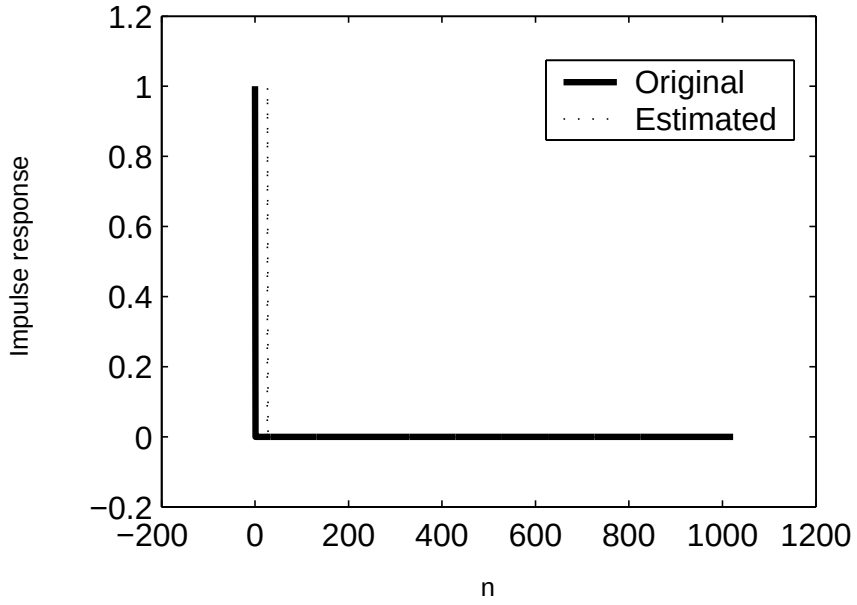

Figure 6.9: Estimated echo path by CMFB when the echo path is purely an impulse.

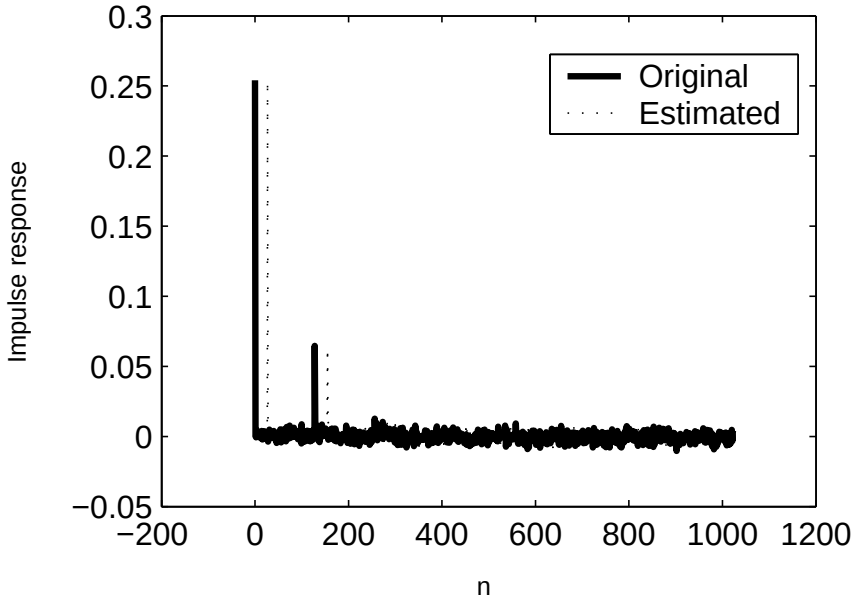

Figure 6.10: Estimated echo path by CMFB when the echo path is adopted from G.168.

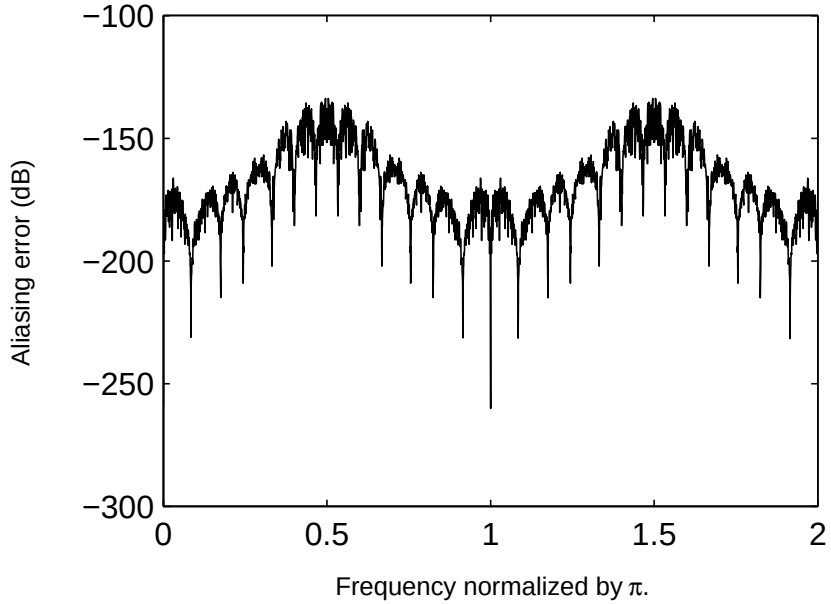

Figure 6.11: Aliasing transfer function for CMFB when the estimated echo path is an impulse.

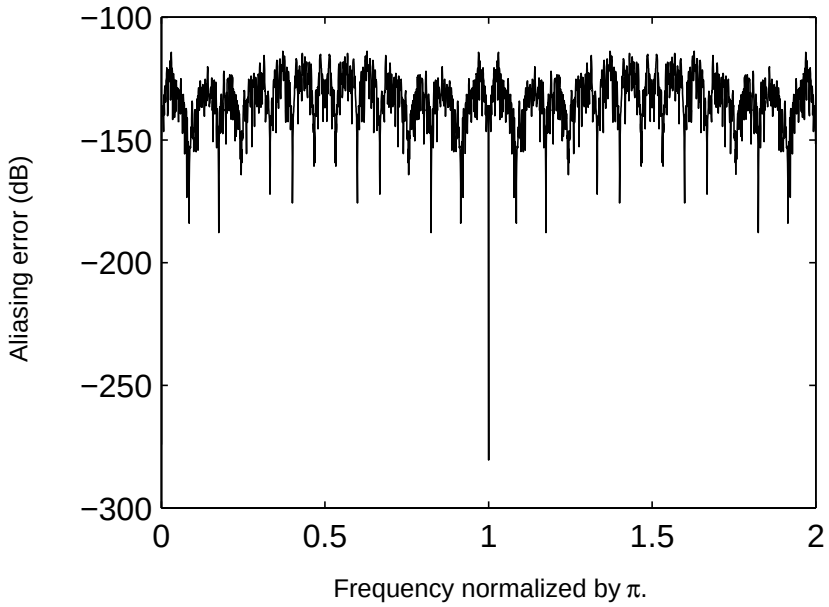

Figure 6.12: Aliasing transfer function for CMFB when the estimated echo path is adopted from G.168.

6.4 Comparison CMFB with the other methods in MSE learning curve

In the following, we examine the acoustic echo cancelation for two echo path models by the learning curve. According to the simulation in [19], the environment setup is with -30dB system noise level or with system noise absent. In our simulation, we set the SNR at the output terminal of the echo path equal to 20dB, 30dB, 40dB, and ∞ (noise absent). We examine the convergence behavior for all methods we have mentioned in the previous section at different SNR values.

First we consider that the echo path model is purely an impulse, which is used in the simulations in [18]. The simulation results are shown in Fig. 6.13. From these figures, CMFB outperforms in mean-squared error values than all the other methods for all iterations. Then we use the the echo path adopted from ITU-T Recommendation G.168. From simulation results, for the SNR levels equal to 20dB and 30dB, CMFB has the smallest MSE value during all iterations, as shown in Fig. 6.14 (a) and (b). CMFB has good convergence behavior for SNR values equal to 20dB and 30dB. As the SNR increases to 40dB and infinity SNR (noise absent), the simulation results are shown in Fig. 6.14 (c) and (d). CMFB can achieve -40dB MSE with only 13000 iterations, while Block DFT achieves -40dB MSE with 20000 iterations. CMFB still has good performance for its fast convergence behavior. For example, suppose the sampling rate is fixed at 8000 Hz. The CMFB achieves an MSE of -40dB faster than Block DFT for 0.875 seconds.

We increase the subband number from 4 to 8. The simulation results are shown in Fig. 6.15 and Fig. 6.16. Compared the simulation results with 4 subbands, the simulation results with 8 subbands demonstrate faster convergence speed. Furthermore, we change the echo path with the room impulse response rir.m. It can be downloaded from MATLAB file exchange center. Fig. 6.17 and Fig. 6.18 show the simulation results with 4 and 8 subbands, respectively. The proposed CMFB still has good convergence performance.

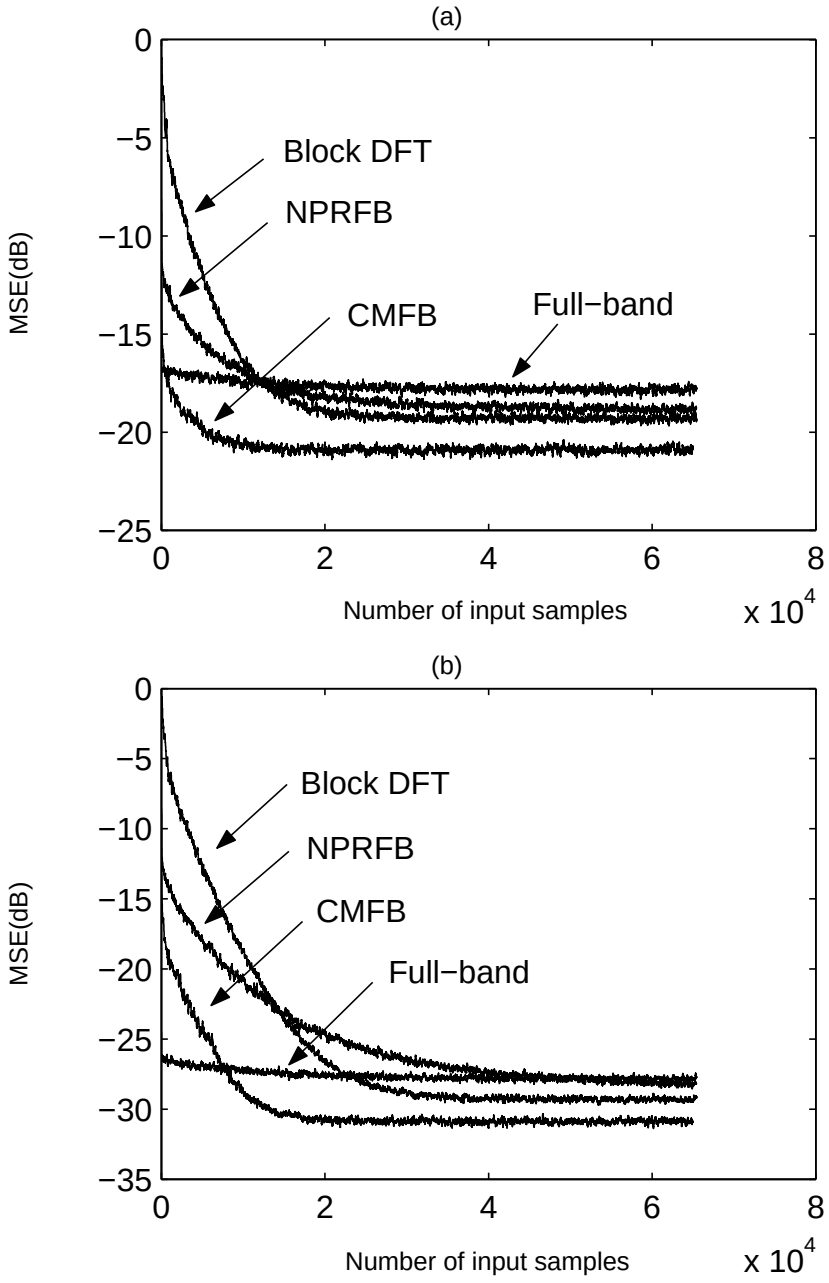
(a)
MSE(dB)
0
−5
−10
−15
−20
−25
Block DFT
NPRFB
CMFB
Full−band
0
2
4
6
8
Number of input samples
x 10^4
(b)
MSE(dB)
0
−5
−10
−15
−20
−25
−30
−35
Block DFT
NPRFB
CMFB
Full−band
0
2
4
6
8
Number of input samples
x 10^4

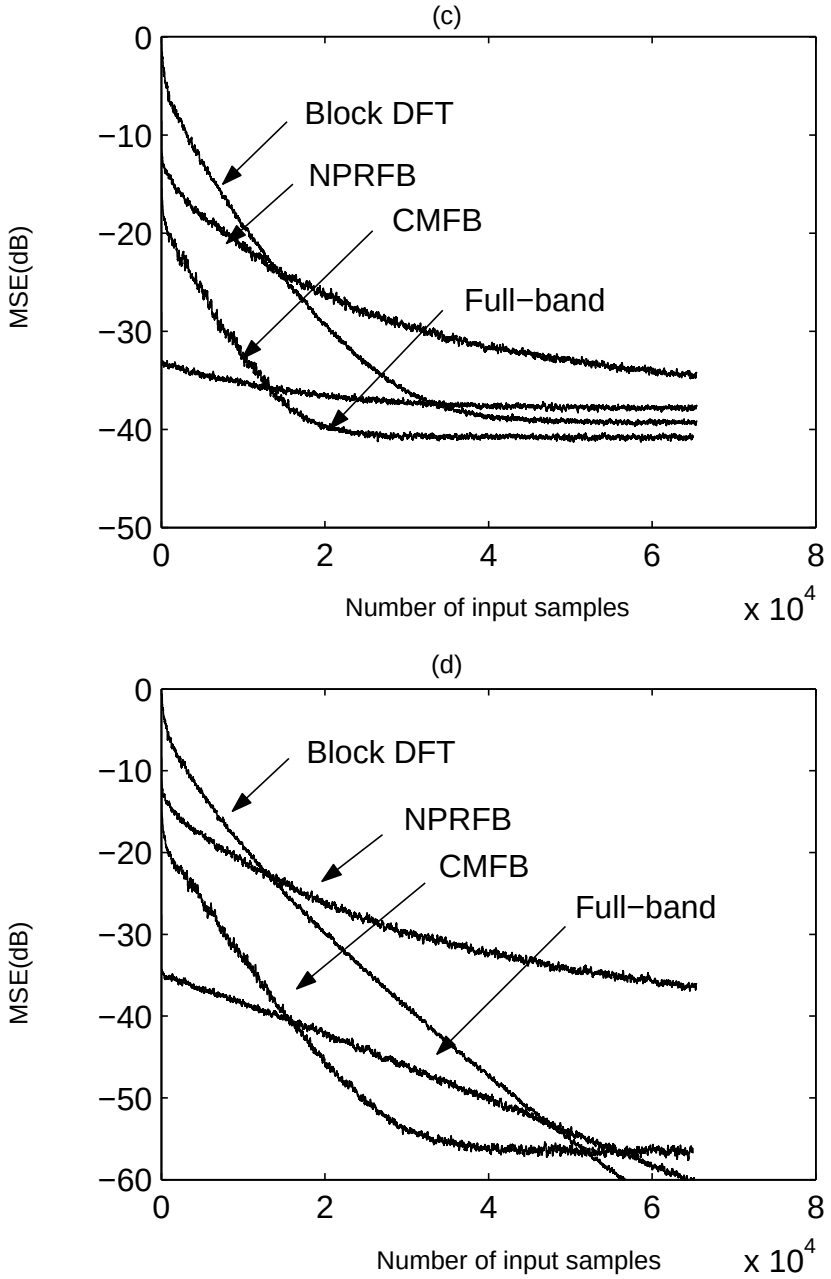

Figure 6.13: Learning curve under different SNR levels with 4 subbands when the echo path is an impulse. (a) SNR = 20dB (b) SNR = 30dB (c) SNR = 40dB (d) SNR = ∞.

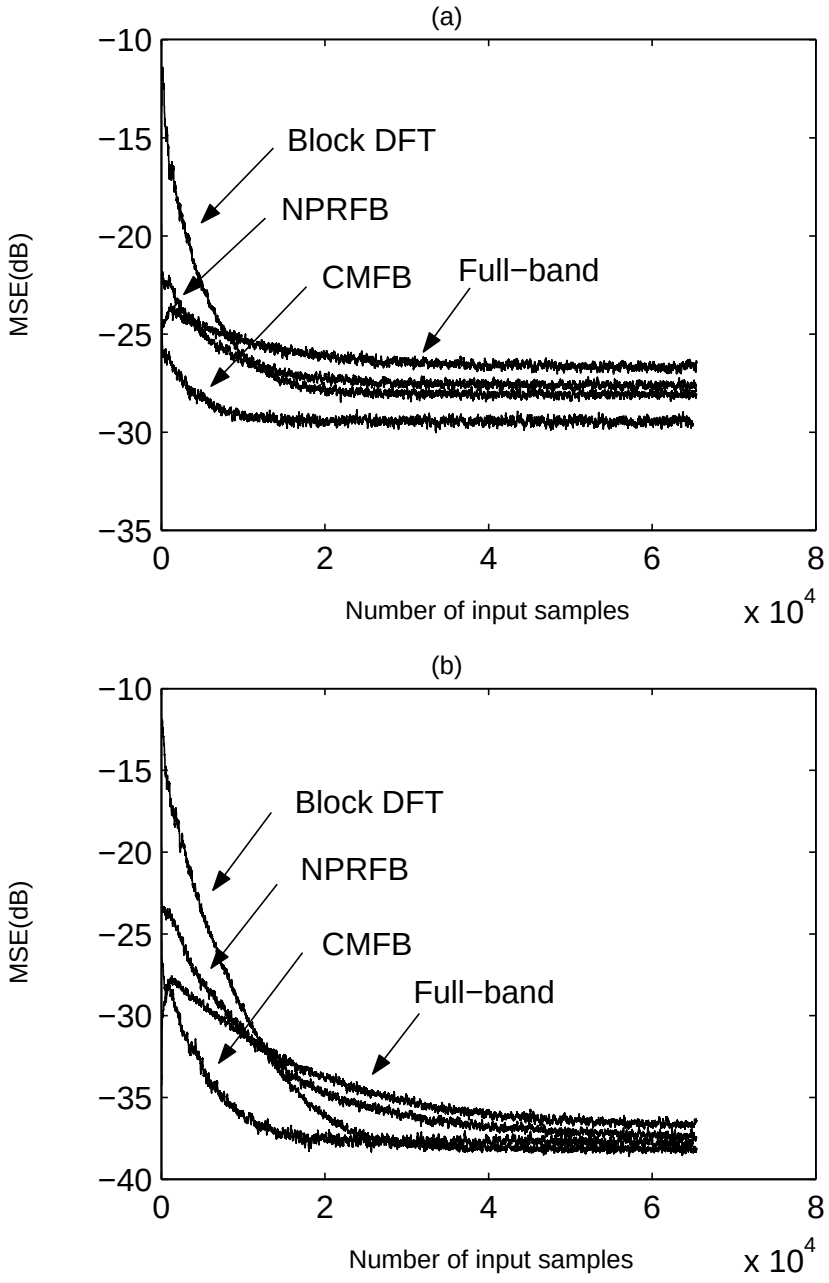
(a)
−10
−15
−20
−25
−30
−35
MSE(dB)
Block DFT
NPRFB
CMFB
Full−band
0
2
4
6
8
Number of input samples
x 10^4
(b)
−10
−15
−20
−25
−30
−35
−40
MSE(dB)
Block DFT
NPRFB
CMFB
Full−band
0
2
4
6
8
Number of input samples
x 10^4

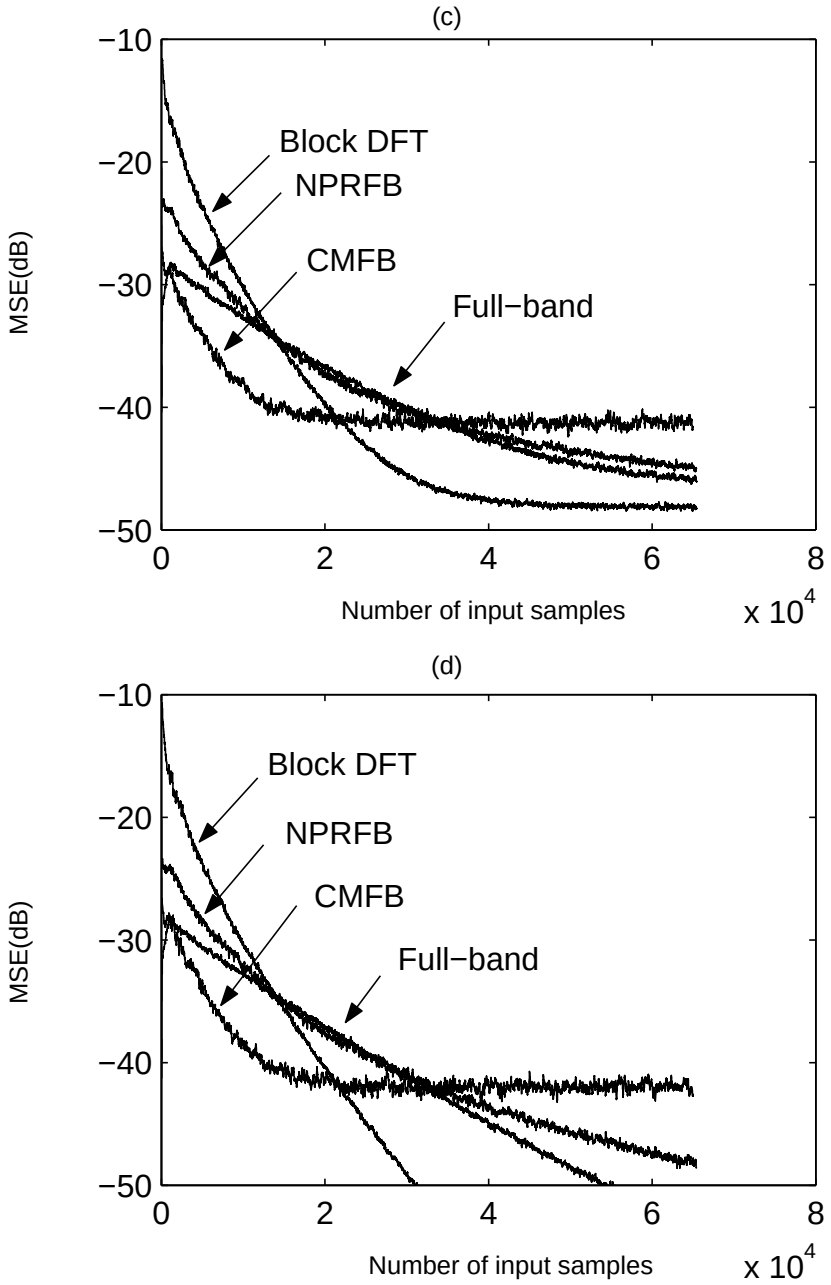

Figure 6.14: Learning curve under different SNR levels with 4 subbands when the echo path is adopted from G.168. (a) SNR = 20dB (b) SNR = 30dB (c) SNR = 40dB (d) SNR = ∞.

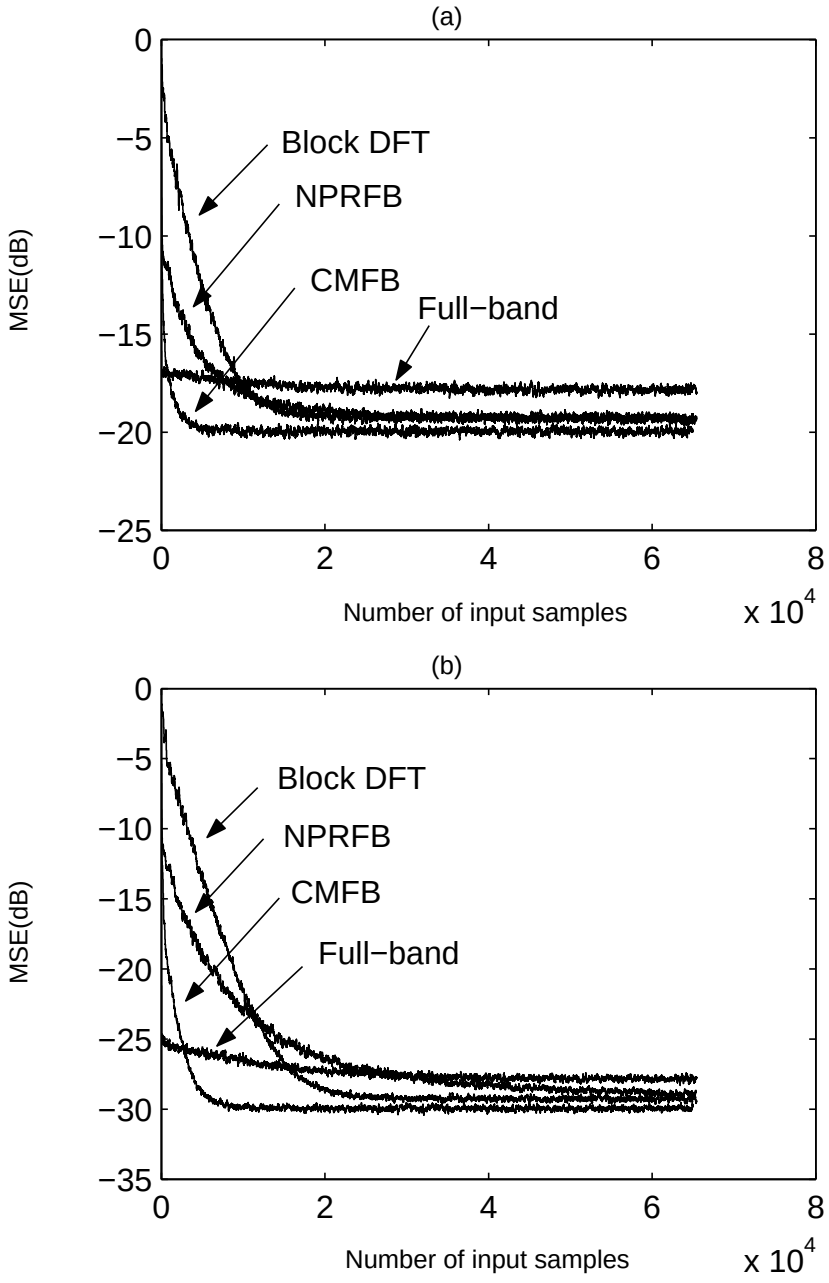
(a)
MSE(dB)
0
−5
−10
−15
−20
−25
Block DFT
NPRFB
CMFB
Full−band
0
2
4
6
8
Number of input samples
x 10^4
(b)
MSE(dB)
0
−5
−10
−15
−20
−25
−30
−35
Block DFT
NPRFB
CMFB
Full−band
0
2
4
6
8
Number of input samples
x 10^4

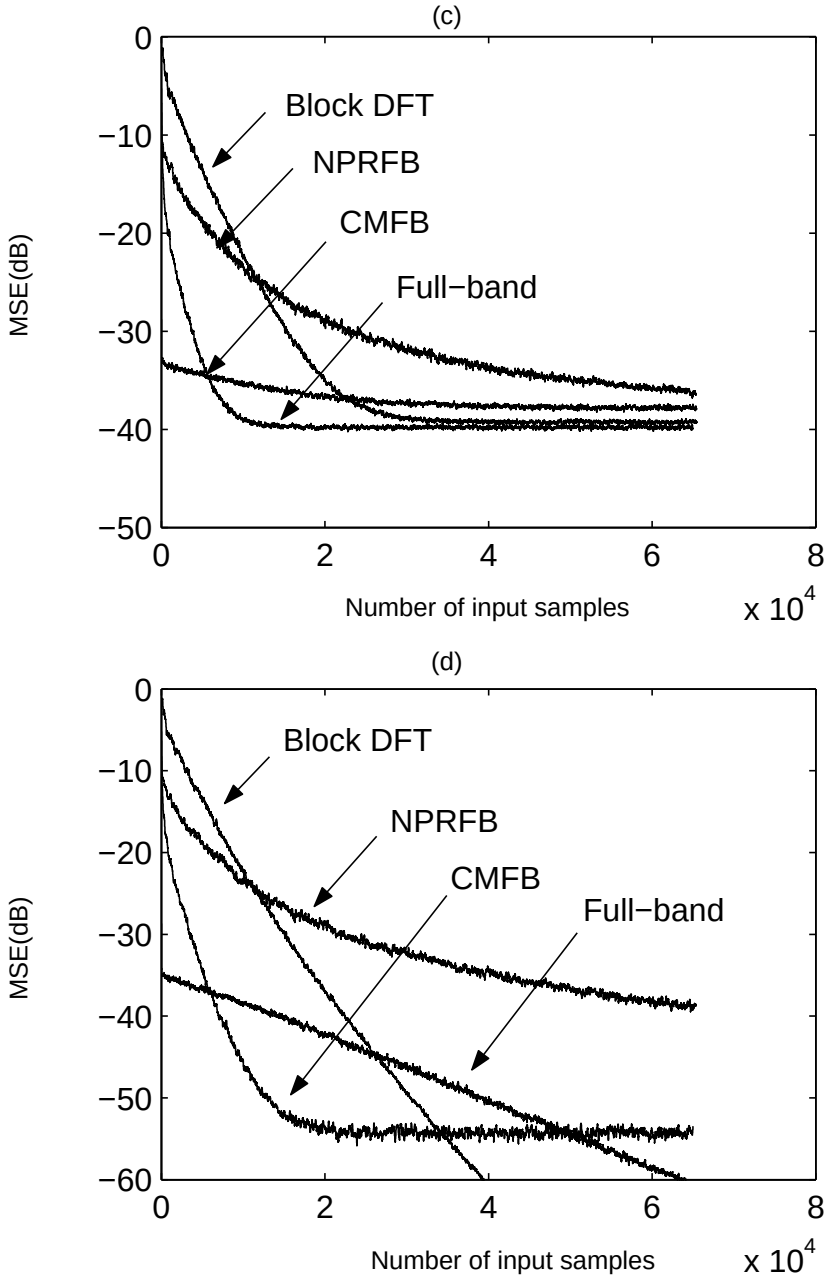

Figure 6.15: Learning curve under different SNR levels with 8 subbands when the echo path is an impulse. (a) SNR = 20dB (b) SNR = 30dB (c) SNR = 40dB (d) SNR = ∞.

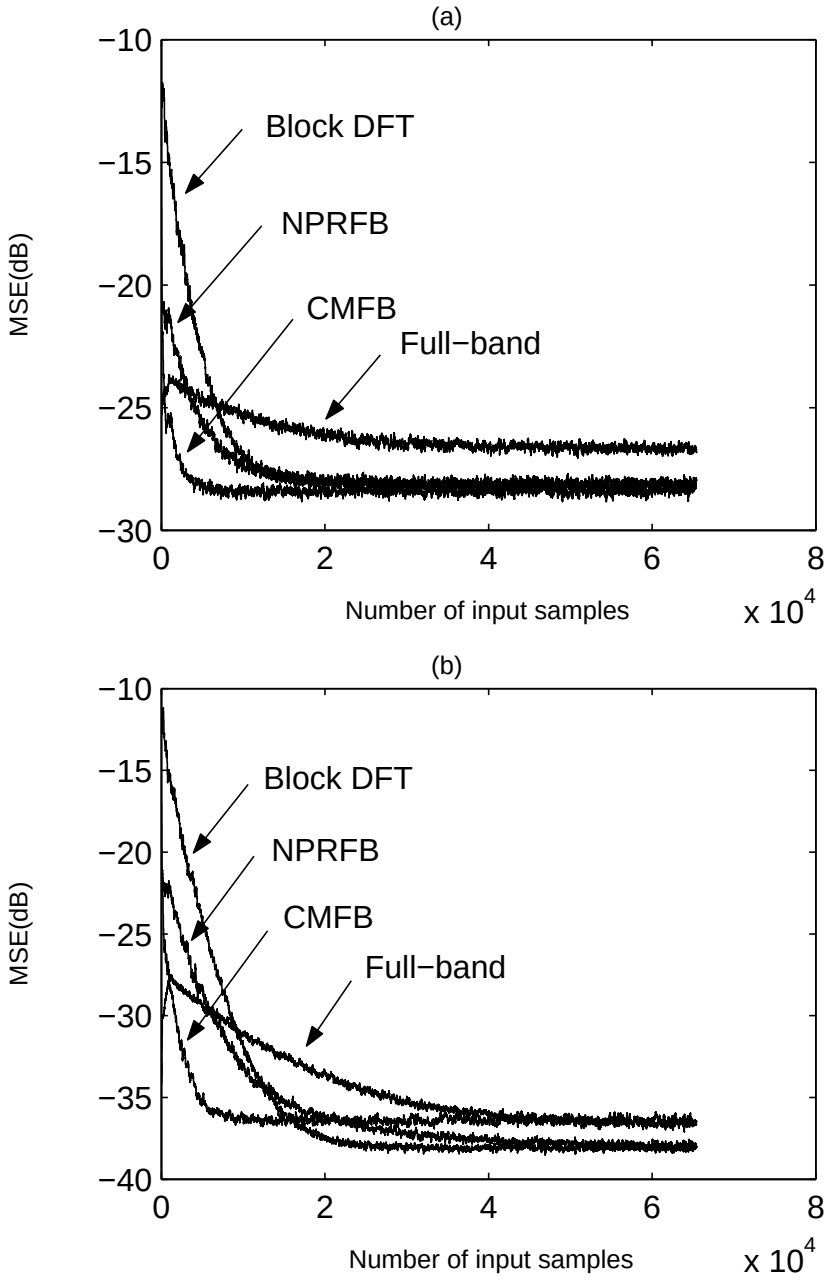
(a)
−10
−15
−20
−25
−30
MSE(dB)
Block DFT
NPRFB
CMFB
Full−band
0
2
4
6
8
Number of input samples
x 10^4
(b)
−10
−15
−20
−25
−30
−35
−40
MSE(dB)
Block DFT
NPRFB
CMFB
Full−band
0
2
4
6
8
Number of input samples
x 10^4

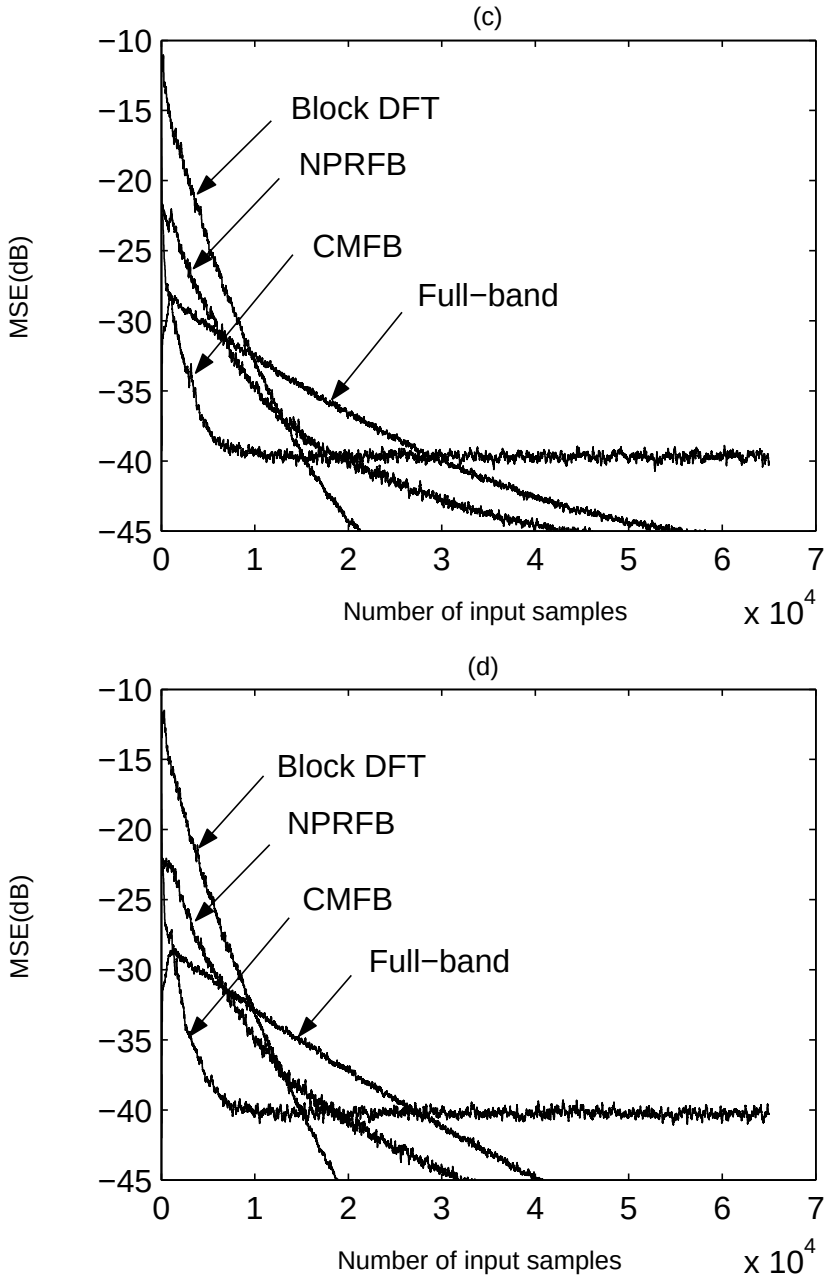

Figure 6.16: Learning curve under different SNR levels with 8 subbands when the echo path is adopted from G.168. (a) SNR = 20dB (b) SNR = 30dB (c) SNR = 40dB (d) SNR = ∞.

(a)

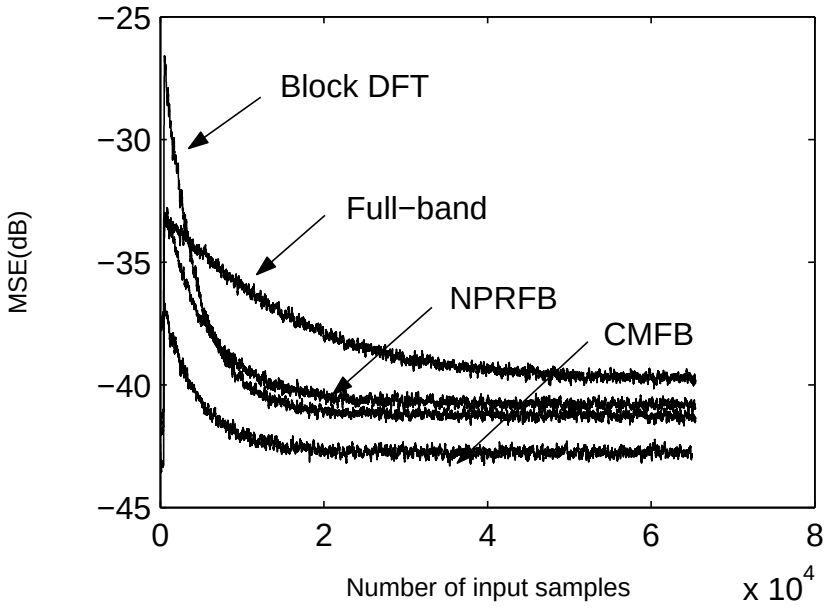
−25
−30
−35
−40
−45
MSE(dB)
Block DFT
Full−band
NPRFB
CMFB
0
2
4
6
8
Number of input samples
x 10^4

(b)

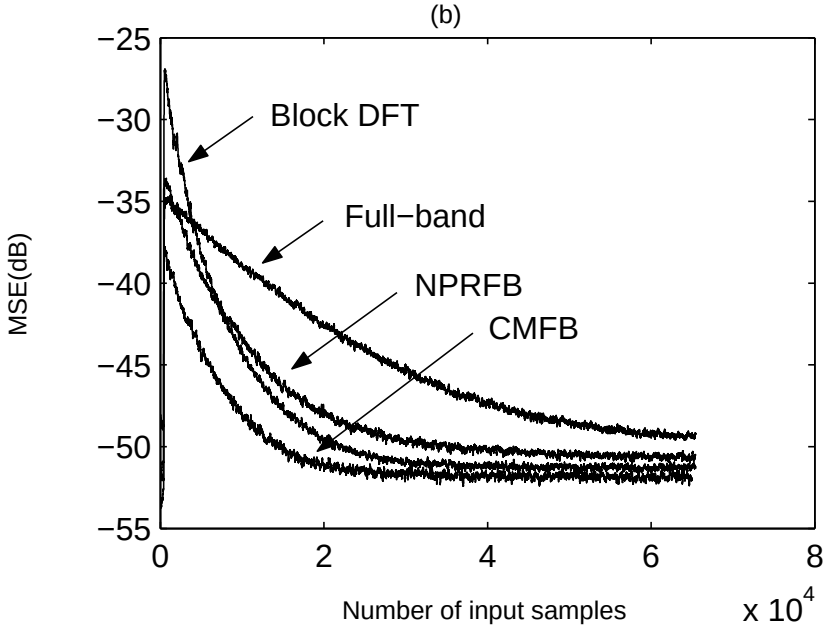
−25
−30
−35
−40
−45
−50
−55
MSE(dB)
Block DFT
Full−band
NPRFB
CMFB
0
2
4
6
8
Number of input samples
x 10^4

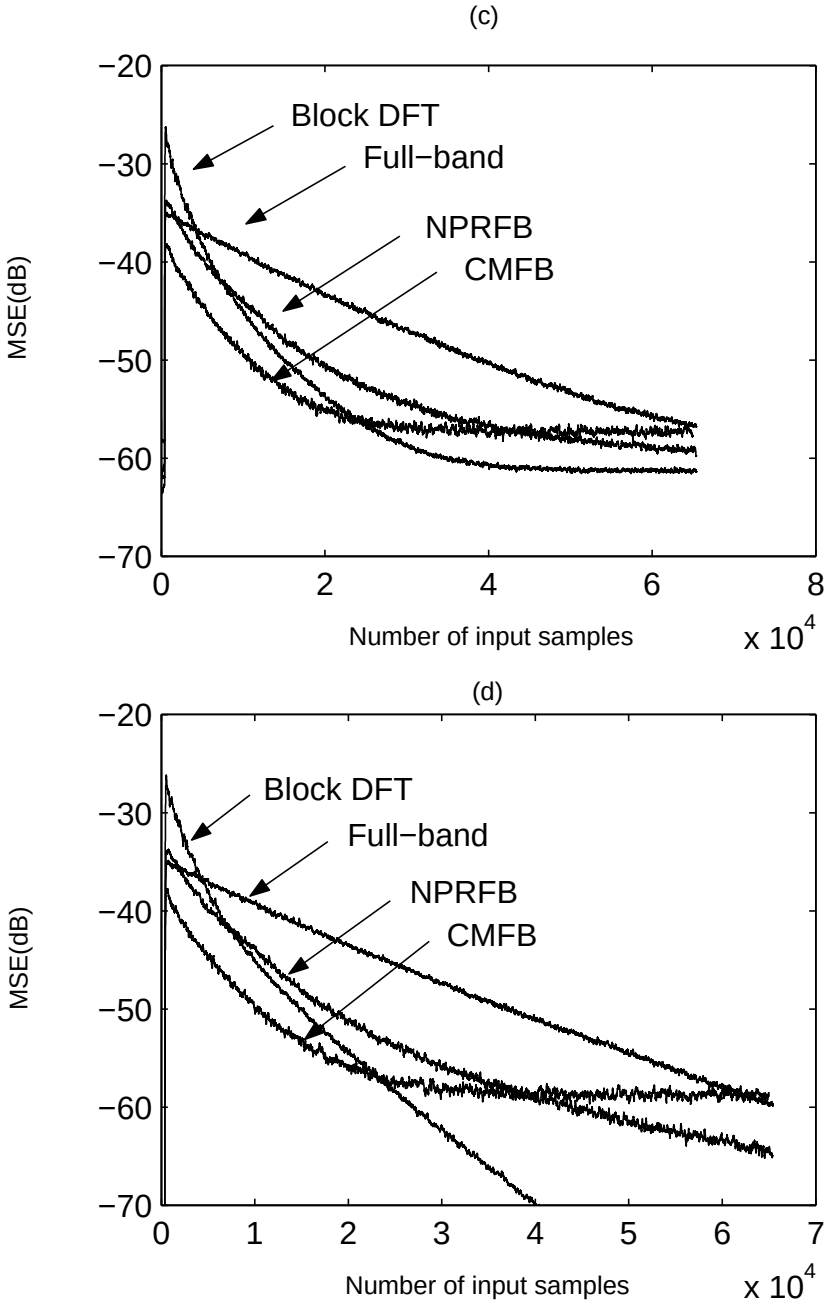

Figure 6.17: Learning curve under different SNR levels with 4 subbands when the echo path is the room impulse response. (a) SNR = 20dB (b) SNR = 30dB (c) SNR = 40dB (d) SNR = ∞.

(a)

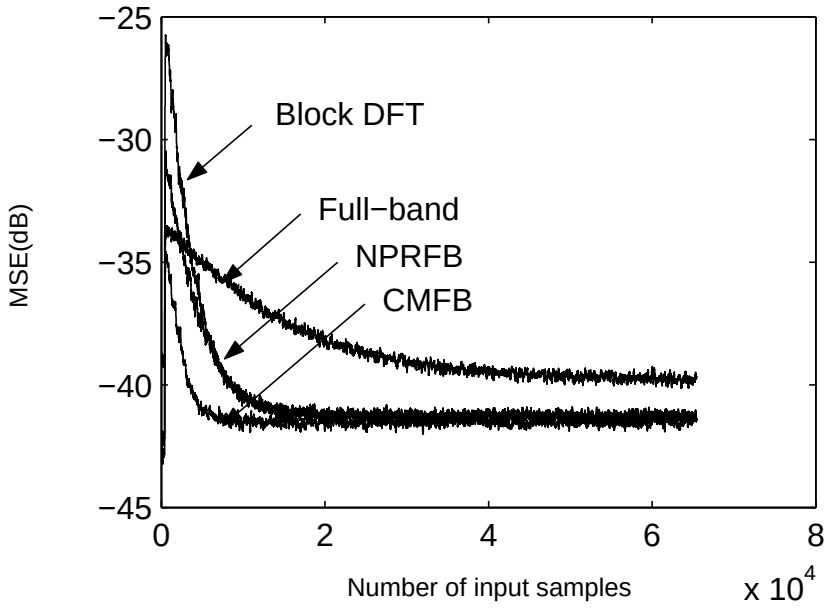
−25
−30
−35
−40
−45
MSE(dB)
Block DFT
Full−band
NPRFB
CMFB
0
2
4
6
8
Number of input samples
x 10^4

(b)

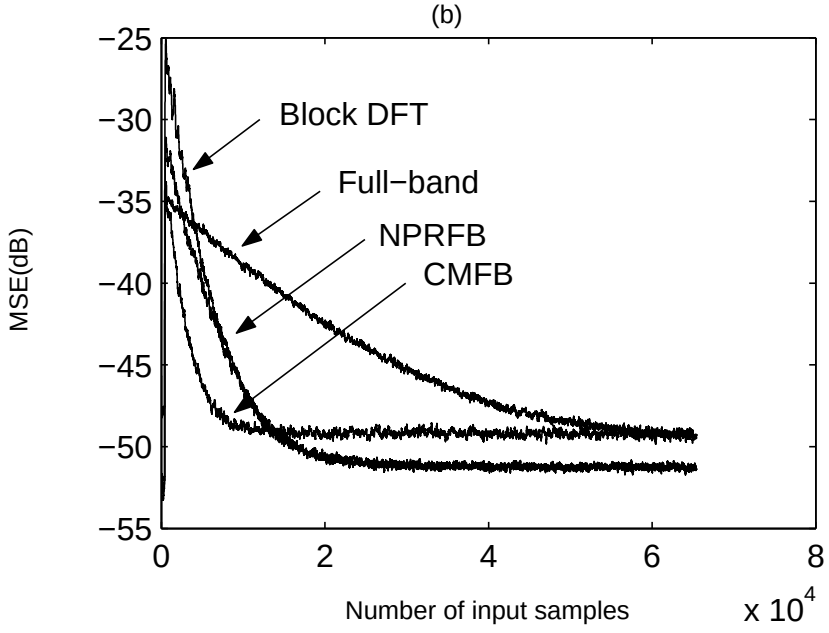
−25
−30
−35
−40
−45
−50
−55
MSE(dB)
Block DFT
Full−band
NPRFB
CMFB
0
2
4
6
8
Number of input samples
x 10^4

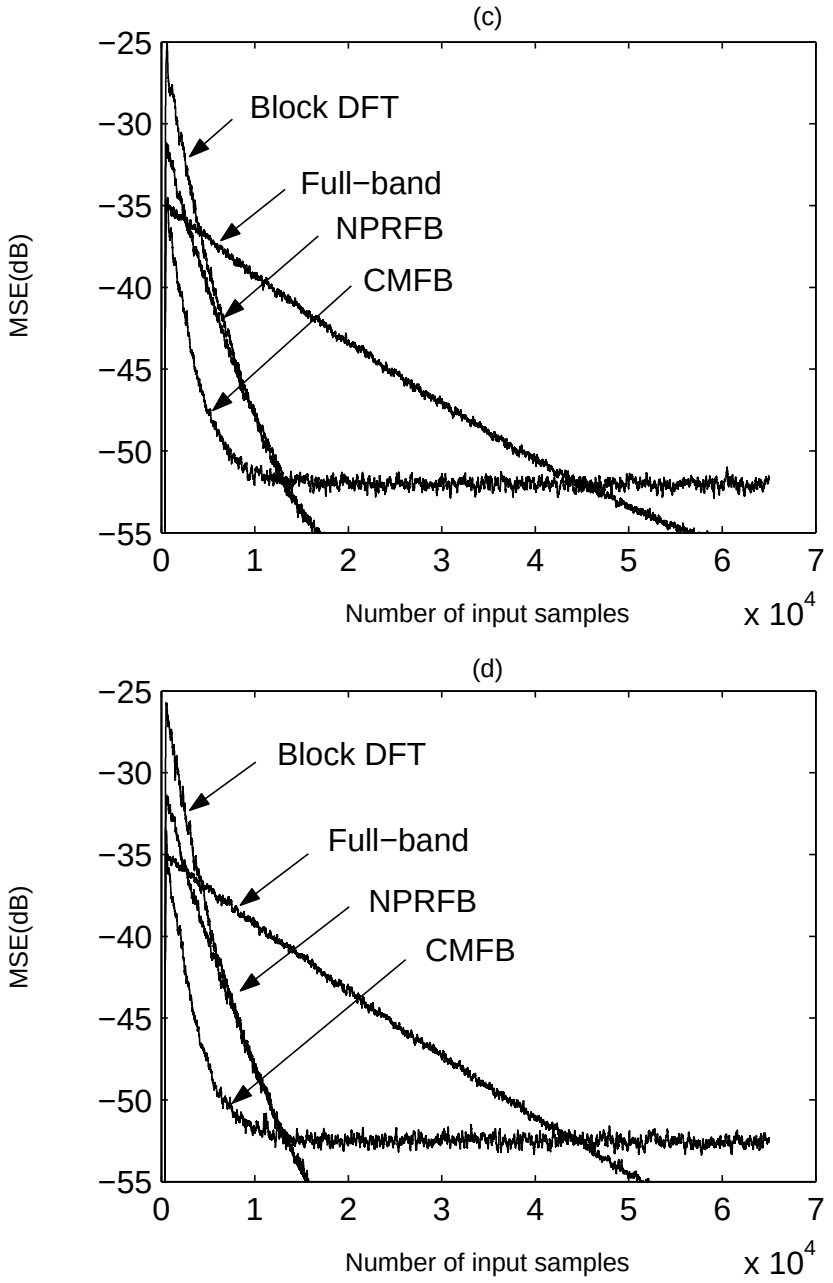

Figure 6.18: Learning curve under different SNR levels with 8 subbands when the echo path is the room impulse response. (a) SNR = 20dB (b) SNR = 30dB (c) SNR = 40dB (d) SNR = ∞.

Chapter 7

Conclusion

In this paper, we proposes an oversampled cosine modulated filterbank (CMFB) for subband adaptive filtering. The filter bank has the approximately alias-free property even in the presence of subband filters. With real-coefficient analysis, synthesis and subband filters, only real additions and multiplications are needed. Furthermore, only half the subband filters need adaptation and the second half can be directly obtained from the first half of the subband filters. Simulation results corroborate that the aliasing error is very close to zero. The learning curves demonstrate that the proposed subband CMFB achieves a small MSE with a fast convergence speed.

Bibliography

[1] S. Haykin, Adaptive Filter Theory, 3nd ed., Prentice-Hall, Englewood Cliffs, New Jersey, 1996.

[2] W. Kellermann, "Analysis and design of multirate systems for cancellation of acoustical echoes," Proc. ICASSP 1988, vol. 5, pp. 2570-2573, 1988.

[3] Gilloire, and M. Vetterli, "Adaptive filtering in subbands with critical sampling: analysis, experiments and application to acoustic echo cancellation," IEEE Trans. Signal Processing, vol. 40, no. 8, pp. 1862-1875, Aug. 1992.

[4] M. R. Petraglia and S. K. Mitra, "Performance analysis of adaptive filter structures based on subband decomposition," Proc. IEEE Int. Symp. Circ. Syst., pp. 60-63, May 1993.

[5] M. R. Petraglia and P. R. V. Piber, "Prototype filter design for oversampled subband adaptive filtering structures," Proc. ISCAS'99, vol. 3, pp. 138-141, 1999.

[6] M. Harteneck, S. Weiss and R. W. Stewart, "Design of near perfect reconstruction oversampled filter banks for subband adaptive filters," IEEE Trans. Circuits and Systems, vol. 46, pp. 1081-1085, 1999.

[7] J. M. de Haan, N. Grbic, I. Claesson, and S. Nordholm, "Design of oversampled uniform DFT filter banks with delay specification using quadratic optimization," Proc. ICASSP, 2001.

[8] N. Grbic, J. M. de Haan, I. Claesson, S. Nordholm, "Design of oversampled uniform DFT filter banks with reduced inband aliasing and delay con-

straints," Signal Processing and its Applications, Sixth International, Symposium on. vol. 1, pp. 104-107, Aug. 2001.

[9] Hai Huyen Dam, Sven Nordholm, Senior Member, IEEE, and Antonio Cantoni, Fellow, IEEE, "Uniform FIR Filterbank Optimization With Group Delay Specifications," IEEE Tran. Signal Processing, vol. 53, no. 11, pp. 4249-4260, Nov. 2005.

[10] K. F. C. Yiu, N. Grbic, S. Nordholm, Kok Lay Teo, "Multicriteria design of oversampled uniform DFT filter banks," IEEE Signal Processing Letters, vol. 11, Issue 6, pp. 541-544, June 2004.

[11] Y.-P. Lin and P. P.Vaidyanathan, "Application of DFT filter banks and cosine modulated filter banks in filtering," Proc. IEEE Asia-Pacific Conference on Circuits and Systems, Dec., 1994.

[12] Y.-P. Lin, and P. P. Vaidyanathan, "A Kaiser Window Approach to the Design of Prototype Filters of Cosine Modulated Filter Banks," IEEE Signal Processing Letters, pp. 132-134, June, 1998.

[13] D. R. Morgan, "Slow asymptotic convergence of LMS acoustic echo cancellers," IEEE Trans. Speech and Audio Processing, Vol. 3, No. 2, March 1995, pp. 126-136.

[14] A. H. Sayed, Fundamentals of Adaptive Filtering, Wiley, 2003.

[15] R. Merched and A. H. Sayed, "An embedding approach to frequency-domain and subband adaptive filtering," IEEE Trans. Signal Processing, vol. 48, no. 9, pp. 2607-2619, 2000.

[16] A. V. Oppenheim and R. W. Schafer, Discrete-Time Signal Processing, Prentice-Hall, Englewood Cliffs, New Jersey, 1989.

[17] P. P. Vaidyanathan, Multirate Systems and Filter Banks. Englewood Cliffs, NJ: Prentice-Hall, 1993.

[18] S. Weiss et al., "Steady-State Perfomauce Limitations of Subband Adaptive Filters," IEEE Trans. on Signal Processing, vol. 49, No. 9, pp. 1982-1990, Sept. 2001.

[19] S. Sandeep Pradhan and V. U. Reddy, "A new approach to subband adaptive filtering, IEEE Trans. on Signal Processing, vol. 47, No. 3, pp. 655-664, Mar. 1999.